
FakeEdge: Alleviate Dataset Shift in Link Prediction

Anonymous Author(s)

Anonymous Affiliation

Anonymous Email

Abstract

Link prediction is a crucial problem in graph-structured data. Due to the recent success of graph neural networks (GNNs), a variety of GNN-based models were proposed to tackle the link prediction task. Specifically, GNNs leverage the message passing paradigm to obtain node representation, which relies on link connectivity. However, in a link prediction task, links in the training set are always present while ones in the testing set are not yet formed, resulting in a discrepancy of the connectivity pattern and bias of the learned representation. It leads to a problem of dataset shift which degrades the model performance. In this paper, we first identify the dataset shift problem in the link prediction task and provide theoretical analyses on how existing link prediction methods are vulnerable to it. We then propose FakeEdge, a model-agnostic technique, to address the problem by mitigating the graph topological gap between training and testing sets. Extensive experiments demonstrate the applicability and superiority of FakeEdge on multiple datasets across various domains.

1 Introduction

Graph structured data is ubiquitous across a variety of domains, including social networks [1], protein-protein interactions [2], movie recommendations [3], and citation networks [4]. It provides a non-Euclidean structure to describe the relations among entities. The link prediction task is to predict missing links or new forming links in an observed network [5]. Recently, with the success of graph neural networks (GNNs) for graph representation learning [6–9], several GNN-based methods have been developed [10–14] to solve link prediction tasks. These methods encode the representation of target links with the topological structures and node/edge attributes in their local neighborhood. After recognizing the pattern of observed links (training sets), they predict the likelihood of forming new links between node pairs (testing sets) where no link is yet observed.

Nevertheless, existing methods pose a discrepancy of the target link representation between training and testing sets. As the target link is never observed in the testing set by the nature of the task, it will have a different local topological structure when compared to its counterpart from the training set. Thus, the corrupted topological structure shifts the target link representation in the testing set, which we recognize it as a dataset shift problem [15, 16] in link prediction. *Note that there are some existing work [11] applying edge masking to moderate such a problem, similar to our treatment. However, they tend to regard it as an empirical trick and fail to identify the fundamental cause as a problem of dataset shift.*

We give a concrete example to illustrate how dataset shift can happen in the link prediction task, especially for GNN-based models with message passing paradigm [17] simulating the 1-dimensional Weisfeiler-Lehman (1-WL) test [18]. In Figure 1, we have two local neighborhoods sampled as subgraphs from the training (top) and testing (bottom) set respectively. The node pairs of interest, which we call focal node pairs, are denoted by black bold circles. From a bird’s-eye viewpoint, these two subgraphs are isomorphic when we consider the existence of the positive test link (dashed line), even though the test link has not been observed. Ideally, two isomorphic graphs should have the same representation encoded by GNNs, leading to the same link prediction outcome. However, one iteration of 1-WL in Figure 1 produces different colors for the focal node pairs between training and

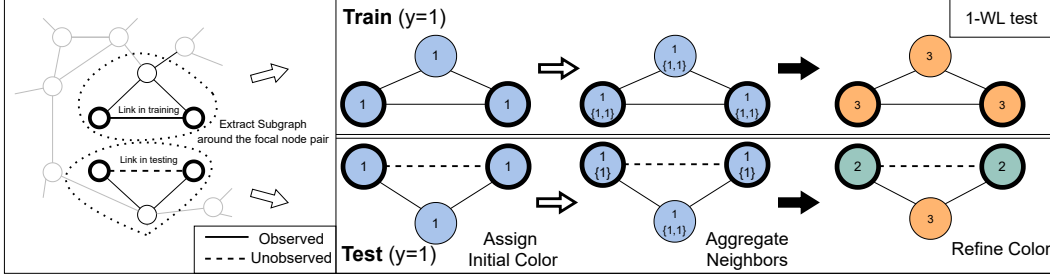


Figure 1: 1-WL test is performed to exhibit the learning process of GNNs. Two node pairs (denoted as bold black circles) and their surrounding subgraphs are sampled from the graph as a training (top) and testing (bottom) instance respectively. Two subgraphs are isomorphic when we omit the focal links. One iteration of 1-WL assigns different colors, indicating the occurrence of dataset shift.

43 testing sets, which indicates that the one-layer GNN can encode different representations for these
 44 two isomorphic subgraphs, giving rise to dataset shift issue.

45 Dataset shift can substantially degrade model performance since it violates the common assumption
 46 that the joint distribution of inputs and outputs stays the same in both the training and testing set. The
 47 root cause of this phenomenon in link prediction is the unique characteristic of the target link: the
 48 link always plays a dual role in the problem setting and determines both the input and the output for a
 49 link prediction task. The existence of the link apparently decides whether it is a positive or negative
 50 sample (output). Simultaneously, the presence of the link can also influence how the representation is
 51 learned through the introduction of different topological structures around the link (input). Thus, it
 52 entangles representation learning and labels in the link prediction problem.

53 To decouple the dual role of the link, we advocate a framework, namely **subgraph link prediction**,
 54 which disentangles the label of the link and its topological structure. As most practical link prediction
 55 methods make a prediction by capturing the local neighborhood of the link [1, 11, 12, 19, 20], we
 56 unify them all into this framework, where the input is the extracted subgraph around the focal node
 57 pair and the output is the likelihood of forming a link incident with the focal node pair in the subgraph.
 58 From the perspective of the framework, we find that the dataset shift issue is mainly caused by the
 59 presence/absence of the focal link in the subgraph from the training/testing set. This motivates us
 60 to propose a simple but effective technique, **FakeEdge**, to deliberately add or remove the focal link
 61 in the subgraph so that the subgraph can stay consistent across training and testing. FakeEdge is a
 62 model-agnostic technique, allowing it to be applied to any subgraph link prediction model. It assures
 63 that the model would learn the same subgraph representation regardless of the existence of the focal
 64 link. Lastly, empirical experiments prove that diminishing the dataset shift issue can significantly
 65 boost the link prediction performance on different baseline models.

66 We summarize our contributions as follows. We first unify most of the link prediction methods into a
 67 common framework named as subgraph link prediction, which treats link prediction as a subgraph
 68 classification task. In the view of the framework, we theoretically investigate the dataset shift issue
 69 in link prediction tasks, which motivates us to propose FakeEdge, a model-agnostic augmentation
 70 technique, to ease the distribution gap between the training and testing. We further conduct extensive
 71 experiments on a variety of baseline models to reveal the performance improvement with FakeEdge
 72 to show its capability of alleviating the dataset shift issue on a broad range of benchmarks.

73 2 Related work

74

75 **Dataset Shift.** Dataset shift is a fundamental issue in the world of machine learning. Within the
 76 collection of dataset shift issues, there are several specific problems based on which part of the data
 77 experience the distributional shift, including covariate shift, concept shift, and prior probability shift.
 78 [16] gives a rigorous definition about different dataset shift situations. In the context of GNNs, [21]
 79 investigates the generalization ability of GNN models, and propose a self-supervised task to improve
 80 the size generalization. [22] studies the problem that the node labels in training set are not uniformly
 81 sampled and suggests applying a regularizer to reduce the distributional gap between training and
 82 testing. [23] proposes a risk minimization method by exploring multiple context of the observed

83 graph to enable GNNs to generalize to out-of-distribution data. [24] demonstrates that the existing
 84 link prediction models can fail to generalize to testing set with larger graphs and designs a structural
 85 pairwise embedding to achieve size stability. [25–27] study the dataset shift problem for graph-level
 86 tasks, especially focusing on the graphs in the training and testing set with varying sizes.

87 **Graph Data Augmentation.** Several data augmentation methods are introduced to modify the
 88 graph connectivity by adding or removing edges [28]. DropEdge [29] acts like a message passing
 89 reducer to tackle over-smoothing or overfitting problems [30]. Topping et al. modify the graph’s
 90 topological structure by removing negatively curved edges to solve the bottleneck issue [32] of
 91 message passing [31]. GDC [33] applies graph diffusion methods on the observed graph to generate
 92 a diffused counterpart as the computation graph. For the link prediction task, CFLP [34] generates
 93 counterfactual links to augment the original graph. Edge Proposal Set [35] injects edges into the
 94 training graph, which are recognized by other link predictors in order to improve performance.

95 3 A proposed unified framework for link prediction

96 In this section, we formally introduce the link prediction task and formulate several existing GNN-
 97 based methods into a common general framework.

98 3.1 Preliminary

99 Let $\mathcal{G} = (V, E, \mathbf{x}^V, \mathbf{x}^E)$ be an undirected graph. V is the set of nodes with size n , which can be
 100 indexed as $\{i\}_{i=1}^n$. $E \subseteq V \times V$ is the observed set of edges. $\mathbf{x}_i^V \in \mathcal{X}^V$ represents the feature of node
 101 i . $\mathbf{x}_{i,j}^E \in \mathcal{X}^E$ represents the feature of the edge (i, j) if $(i, j) \in E$. The other unobserved set of edges
 102 is $E_c \subseteq V \times V \setminus E$, which are either missing or going to form in the future in the original graph \mathcal{G} .
 103 $d(i, j)$ denotes the shortest path distance between node i and j . The r -hop *enclosing subgraph* $\mathcal{G}_{i,j}^r$
 104 for node i, j is the subgraph induced from \mathcal{G} by node sets $V_{i,j}^r = \{v | v \in V, d(v, i) \leq r \text{ or } d(v, j) \leq r\}$.
 105 The edges set of $\mathcal{G}_{i,j}^r$ are $E_{i,j}^r = \{(p, q) | (p, q) \in E \text{ and } p, q \in V_{i,j}^r\}$. An enclosing subgraph
 106 $\mathcal{G}_{i,j}^r = (V_{i,j}^r, E_{i,j}^r, \mathbf{x}_{V_{i,j}^r}^V, \mathbf{x}_{E_{i,j}^r}^E)$ contains all the information in the neighborhood of node i, j . The
 107 node set $\{i, j\}$ is called the *focal node pair*, where we are interested in if there exists (observed) or
 108 should exist (unobserved) an edge between nodes i, j . In the context of link prediction, we will use
 109 the term **subgraph** to denote *enclosing subgraph* in the following sections.

110 3.2 Subgraph link prediction

111 In this section, we discuss the definition of **Subgraph Link Prediction** and investigate how current
 112 link prediction methods can be unified in this framework. We mainly focus on link prediction
 113 methods based on GNNs, which propagate the message to each node’s neighbors in order to learn the
 114 representation. We start by giving the definition of the subgraph’s properties:

115 **Definition 1.** Given a graph $\mathcal{G} = (V, E, \mathbf{x}^V, \mathbf{x}^E)$ and the unobserved edge set E_c , a subgraph $\mathcal{G}_{i,j}^r$
 116 have the following properties:

- 117 1. a **label** $y \in \{0, 1\}$ of the subgraph indicates if there exists, or will form, an edge incident with focal
 118 node pair $\{i, j\}$. That is, $\mathcal{G}_{i,j}^r$ label $y = 1$ if and only if $(i, j) \in E \cup E_c$. Otherwise, label $y = 0$.
- 119 2. the **existence** $e \in \{0, 1\}$ of an edge in the subgraph indicates whether there is an edge observed at
 120 the focal node pair $\{i, j\}$. If $(i, j) \in E$, $e = 1$. Otherwise $e = 0$.
- 121 3. a **phase** $c \in \{\text{train}, \text{test}\}$ denotes whether the subgraph belongs to training or testing stage.
 122 Especially for a positive subgraph ($y = 1$), if $(i, j) \in E$, then $c = \text{train}$. If $(i, j) \in E_c$, then $c = \text{test}$.

123 Note that, the *label* $y = 1$ does not necessarily indicate the observation of the edge at the focal node
 124 pair $\{i, j\}$. A subgraph in the testing set may have the label $y = 1$ but the edge may not be present.
 125 The *existence* $e = 1$ only when the edge is observed at the focal node pair.

126 **Definition 2.** Given a subgraph $\mathcal{G}_{i,j}^r$, **Subgraph Link Prediction** is a task to learn a feature \mathbf{h} of the
 127 subgraph $\mathcal{G}_{i,j}^r$ and uses it to predict the label $y \in \{0, 1\}$ of the subgraph.

128 Generally, subgraph link prediction regards the link prediction task as a subgraph classification task.
 129 The pipeline of subgraph link prediction starts with extracting the subgraph $\mathcal{G}_{i,j}^r$ around the focal
 130 node pair $\{i, j\}$, and then applies GNNs to encode the node representation \mathbf{Z} . The latent feature \mathbf{h} of
 131 the subgraph is obtained by pooling methods on \mathbf{Z} . In the end, the subgraph feature \mathbf{h} is fed into a
 132 classifier. In summary, the whole pipeline entails:

- 133 1. **Subgraph Extraction:** Extract the subgraph $\mathcal{G}_{i,j}^r$ around the focal node pair $\{i, j\}$;
- 134 2. **Node Representation Learning:** $\mathbf{Z} = \text{GNN}(\mathcal{G}_{i,j}^r)$, where $\mathbf{Z} \in \mathbb{R}^{|\mathcal{V}_{i,j}^r| \times F_{\text{hidden}}}$ is the node embed-
135 ding matrix learned by the GNN encoder;
- 136 3. **Pooling:** $\mathbf{h} = \text{Pooling}(\mathbf{Z}; \mathcal{G}_{i,j}^r)$, where $\mathbf{h} \in \mathbb{R}^{F_{\text{pooled}}}$ is the latent feature of the subgraph $\mathcal{G}_{i,j}^r$;
- 137 4. **Classification:** $y = \text{Classifier}(\mathbf{h})$.

138 There are two main streams of GNN-based link prediction models. Models like SEAL [11] and
139 WalkPool [12] can naturally fall into the subgraph link prediction framework, as they thoroughly
140 follow the pipeline. In SEAL, SortPooling [36] serves as a readout to aggregate the node’s features in
141 the subgraph. WalkPool designs a random-walk based pooling method to extract the subgraph feature
142 \mathbf{h} . Both methods take advantage of the node’s representation from the entire subgraph.

143 In addition, there is another stream of link prediction models, such as GAE [10] and PLNLP [14],
144 which learns the node representation and then devises a score function on the representation of the
145 focal node pair to represent the likelihood of forming a link. We find that these GNN-based methods
146 with the message passing paradigm also belong to a subgraph link prediction task. Considering a
147 GAE with l layers, each node v essentially learns its embedding from its l -hop neighbors $\{i | i \in$
148 $V, d(i, v) \leq l\}$. The score function can be then regarded as a center pooling on the subgraph, which
149 only aggregates the features of the focal node pair as \mathbf{h} to represent the subgraph. For a focal node
150 pair $\{i, j\}$ and GAE with l layers, an l -hop subgraph $\mathcal{G}_{i,j}^l$ sufficiently contains all the information
151 needed to learn the representation of nodes in the subgraph and score the focal node pair $\{i, j\}$. Thus,
152 the GNN-based models can also be seen as a citizen of subgraph link prediction. In terms of the
153 score function, there are plenty of options depending on the predictive power in practice. In general,
154 the common choices are: (1) Hadamard product: $\mathbf{h} = z_i \circ z_j$; (2) MLP: $\mathbf{h} = \text{MLP}(z_i \circ z_j)$ where
155 MLP is the Multi-Layer Perceptron; (3) BiLinear: $\mathbf{h} = z_i \mathbf{W} z_j$ where \mathbf{W} is a learnable matrix; (4)
156 BiLinearMLP: $\mathbf{h} = \text{MLP}(z_i) \circ \text{MLP}(z_j)$.

157 In addition to GNN-based methods, the concept of the subgraph link prediction can be extended to low-
158 order heuristics link predictors, like Common Neighbor [1], Adamic–Adar index [20], Preferential
159 Attachment [37], Jaccard Index [38], and Resource Allocation [39]. The predictors with the order r
160 can be computed by the subgraph $\mathcal{G}_{i,j}^r$. The scalar value can be seen as the latent feature \mathbf{h} .

161 4 FakeEdge: Mitigates dataset shift in subgraph link prediction

162 In this section, we start by giving the definition of dataset shift in the general case, and then formally
163 discuss how dataset shift occurs with regard to subgraph link prediction. Then we propose FakeEdge
164 as a graph augmentation technique to ease the distribution gap of the subgraph representation between
165 the training and testing sets. Lastly, we discuss how FakeEdge can enhance the expressive power of
166 any GNN-based subgraph link prediction model.

167 4.1 Dataset shift

168 **Definition 3.** *Dataset Shift happens when the joint distribution between train and test is different.*
169 *That is, $p(\mathbf{h}, y | c = \text{train}) \neq p(\mathbf{h}, y | c = \text{test})$.*

170 A simple example of dataset shift is an object detection system. If the system is only designed and
171 trained under good weather conditions, it may fail to capture objects in bad weather. In general,
172 dataset shift is often caused by some unknown latent variable, like the weather condition in the
173 example above. The unknown variable is not observable during the training phase so the model
174 cannot fully capture the conditions during testing. Similarly, the edge existence $e \in \{0, 1\}$ in the
175 subgraph poses as an "unknown" variable in the subgraph link prediction task. Most of the current
176 GNN-based models neglect the effect of the edge existence on encoding the subgraph’s feature.

177 **Definition 4.** *A subgraph’s feature \mathbf{h} is called Edge Invariant if $p(\mathbf{h}, y | e) = p(\mathbf{h}, y)$.*

178 To explain, the **Edge Invariant** subgraph embedding stays the same no matter if the edge is present
179 at the focal node pair or not. It disentangles the edge’s existence and the subgraph representation
180 learning. For example, common neighbor predictor is Edge Invariant because the existence of an
181 edge at the focal node pair will not affect the number of common neighbors that two nodes can have.
182 However, Preferential Attachment, another widely used heuristics link prediction predictor, is **not**
183 Edge Invariant because the node degree varies depending on the existence of the edge. **A further**
184 **discussion can be found in Appendix I.**

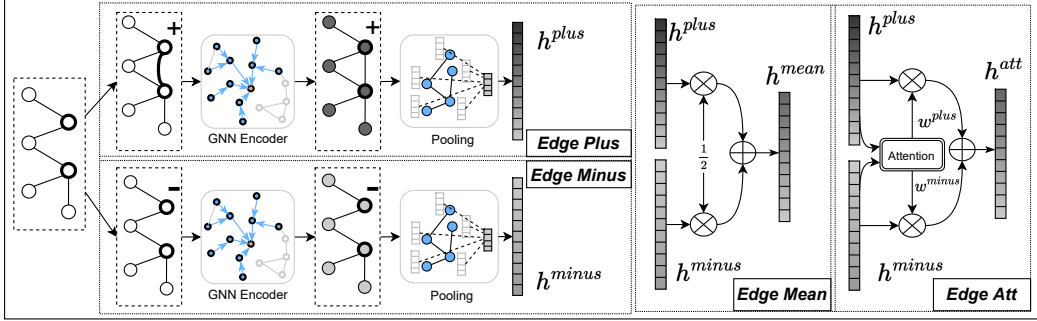


Figure 2: The proposed four FakeEdge methods. In general, FakeEdge encourages the link prediction model to learn the subgraph representation by always deliberately adding or removing the edges at the focal node pair in each subgraph. In this way, FakeEdge can reduce the distribution gap of the learned subgraph representation between the training and testing set.

185 **Theorem 1.** *GNN cannot learn the subgraph feature \mathbf{h} to be Edge Invariant.*

186 Recall that the subgraphs in Figure 1 are encoded differently between the training and testing set
 187 because of the presence/absence of the focal link. Thus, the vanilla GNN cannot learn the Edge
 188 Invariant subgraph feature. Learning Edge Invariant subgraph feature is crucial to mitigate the dataset
 189 shift problem. Here, we give our main theorem about the issue in the link prediction task:

190 **Theorem 2.** *Given $p(\mathbf{h}, y|e, c) = p(\mathbf{h}, y|e)$, there is no Dataset Shift in the link prediction if the*
 191 *subgraph embedding is Edge Invariant. That is, $p(\mathbf{h}, y|e) = p(\mathbf{h}, y) \implies p(\mathbf{h}, y|c) = p(\mathbf{h}, y)$.*

192 The assumption $p(\mathbf{h}, y|e, c) = p(\mathbf{h}, y|e)$ states that when the edge at the focal node pair is taken
 193 into consideration, the joint distribution keeps the same across the training and testing stages, which
 194 means that there is no other underlying unobserved latent variable shifting the distribution. The
 195 theorem shows an **Edge Invariant** subgraph embedding will not cause a dataset shift phenomenon.

196 **Theorem 2** gives us the motivation to design the subgraph embedding to be Edge Invariant. When
 197 it comes to GNNs, the practical GNN is essentially a message passing neural network [17]. The
 198 existence of the edge incident at the focal node pair can determine the computational graph for
 199 message passing when learning the node representation.

200 **4.2 Proposed methods**

201 Having developed conditions of dataset shift phenomenon in link prediction, we next introduce a
 202 collection of subgraph augmentation techniques named as **FakeEdge** (Figure 2), which satisfies
 203 the conditions in Theorem 2. The motivation is to mitigate the distribution shift of the subgraph
 204 embedding by eliminating the different patterns of target link existence between training and testing
 205 sets. Note that all of the strategies follow the same discipline: align the topological structure
 206 around the focal node pair in the training and testing datasets, especially for the isomorphic subgraphs.
 207 Therefore, we expect that it can gain comparable performance improvement across different strategies.

208 Compared to the vanilla GNN-based subgraph link prediction methods, FakeEdge augments the
 209 computation graph for node representation learning and subgraph pooling step to obtain an Edge
 210 Invariant embedding for the entire subgraph.

211 **Edge Plus** A simple strategy is to always make the edge present at the focal node pair for all training
 212 and testing samples. Namely, we add an edge into the edge set of subgraph by $E_{i,j}^{r+} = E_{i,j}^r \cup \{(i, j)\}$,
 213 and use this edge set to calculate the representation \mathbf{h}^{plus} of the subgraph $\mathcal{G}_{i,j}^{r+}$.

214 **Edge Minus** Another straightforward modification is to remove the edge at the focal node pair if
 215 existing. That is, we remove the edge from the edge set of subgraph by $E_{i,j}^{r-} = E_{i,j}^r \setminus \{(i, j)\}$, and
 216 obtain the representation \mathbf{h}^{minus} from $\mathcal{G}_{i,j}^{r-}$.

217 For GNN-based models, adding or removing edges at the focal node pair can amplify or reduce
 218 message propagation along the subgraph. It may also change the connectivity of the subgraph. We
 219 are interested to see if it can be beneficial to take both situations into consideration by combining
 220 them. Based on *Edge Plus* and *Edge Minus*, we further develop another two Edge Invariant methods:

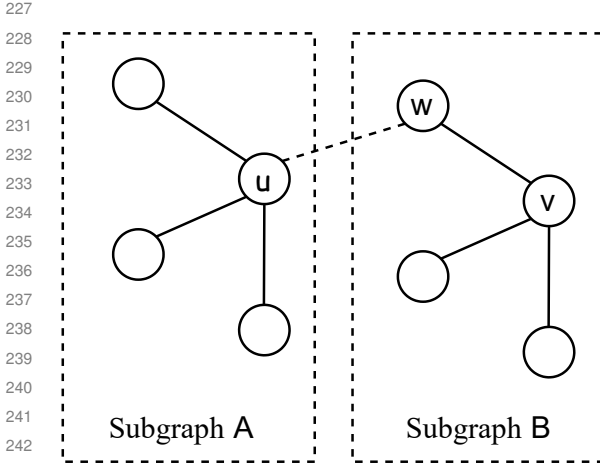
221 **Edge Mean** To combine *Edge Plus* and *Edge Minus*, one can extract these two features and fuse them
 222 into one view. One way is to take the average of the two latent features by $\mathbf{h}^{mean} = \frac{\mathbf{h}^{plus} + \mathbf{h}^{minus}}{2}$.

223 **Edge Att** *Edge Mean* weighs $\mathcal{G}_{i,j}^{r+}$ and $\mathcal{G}_{i,j}^{r-}$ equally on all subgraphs. To vary the importance of two
 224 modified subgraphs, we can apply an adaptive weighted sum operation. Similar to the practice in the
 225 text translation [40], we apply an attention mechanism to fuse the \mathbf{h}^{plus} and \mathbf{h}^{minus} by:

$$\mathbf{h}^{att} = w^{plus} * \mathbf{h}^{plus} + w^{minus} * \mathbf{h}^{minus}, \quad (1)$$

$$\text{where } w = \text{SoftMax}(\mathbf{q}^T \cdot \tanh(\mathbf{W} \cdot \mathbf{h} + \mathbf{b})) \quad (2)$$

226 4.3 Expressive power of structural representation



244 **Figure 3:** Given two isomorphic but non-
 245 overlapping subgraphs *A* and *B*, GNNs learn the
 246 same representation for the nodes *u* and *v*. Hence,
 247 GNN-based methods cannot distinguish focal node
 248 pairs $\{u, w\}$ and $\{v, w\}$. However, by adding a Fake
 249 Edge at $\{u, w\}$ (shown as the dashed line in the
 250 figure), it can break the tie of the representation for
 251 *u* and *v*, thanks to *u*'s modified neighborhood.

In addition to solving the issue of dataset shift, FakeEdge can tackle another problem that impedes the expressive power of link prediction methods on the structural representation [41]. In general, a powerful model is expected to discriminate most of the non-isomorphic focal node pairs. For instance, in Figure 3 we have two isomorphic subgraphs *A* and *B*, which do not have any overlapping nodes. Suppose that the focal node pairs we are interested in are $\{u, w\}$ and $\{v, w\}$. Obviously, those two focal node pairs have different structural roles in the graph, and we expect different structural representations for them. With GNN-based methods like GAE, the node representation of the node *u* and *v* will be the same $z_u = z_v$, due to the fact that they have isomorphic neighborhoods. GAE applies a score function on the focal node pair to pool the subgraph's feature. Hence, the structural representation of node sets $\{u, w\}$ and $\{v, w\}$ would be the same, leaving them inseparable in the embedding space. This issue is caused by the limitation of GNNs, whose expressive power is bounded by 1-WL test [42].

252 Zhang et al. address this problem by assigning distinct labels between the focal node pair and the rest of the nodes in the subgraph [19]. FakeEdge manages to resolve the issue by augmenting the neighborhoods of those two isomorphic nodes. For instance, we can utilize the *Edge Plus* strategy to deliberately add an edge between nodes *u* and *w* (shown as the dashed line in Figure 3). Note that the edge between *v* and *w* has already existed. There is no need to add an edge between them. Therefore, the node *u* and *v* will have different neighborhoods (*u* has 4 neighbors and *v* has 3 neighbors), resulting in the different node representation between the node *u* and *v* after the first iteration of message propagation with GNN. In the end, we can obtain different representations for two focal node pairs. Other FakeEdge methods like *Edge Minus* can also tackle the issue in a similar way.

261 According to Theorem 2 in [19], such non-isomorphic focal node pairs $\{u, w\}$, $\{v, w\}$ are not
 262 sporadic cases in a graph. Given an *n* nodes graph whose node degree is $\mathcal{O}(\log^{\frac{1-\epsilon}{2r}} n)$ for any
 263 constant $\epsilon > 0$, there exists $\omega(n^{2\epsilon})$ pairs of such kind of $\{u, w\}$ and $\{v, w\}$, which cannot be
 264 distinguished by GNN-based models like GAE. However, FakeEdge can enhance the expressive
 265 power of link prediction methods by modifying the subgraph's local connectivity.

266 5 Experiments

267 In this section, we conduct extensive experiments to evaluate how FakeEdge can mitigate the dataset
 268 shift issue on various baseline models in the link prediction task. Then we empirically show the
 269 distribution gap of the subgraph representation between the training and testing and discuss how the
 270 dataset shift issue can worsen with deeper GNNs.

Table 1: Comparison with and without FakeEdge (AUC). The best results are highlighted in bold.

Models	FakeEdge	Cora	Citeseer	Pubmed	USAir	NS	PB	Yeast	C.ele	Power	Router	E.coli
GCN	<i>Original</i>	84.92 \pm 1.95	77.05 \pm 2.18	81.58 \pm 4.62	94.07 \pm 1.50	96.92 \pm 0.73	93.17 \pm 0.45	93.76 \pm 0.65	88.78 \pm 1.85	76.32 \pm 4.65	60.72 \pm 5.88	95.35 \pm 0.36
	<i>Edge Plus</i>	91.94 \pm 0.90	89.54 \pm 1.17	97.91 \pm 0.14	97.10 \pm 1.01	98.03 \pm 0.72	95.48 \pm 0.42	97.86 \pm 0.27	89.65 \pm 1.74	85.42\pm0.91	95.96 \pm 0.41	98.05 \pm 0.30
	<i>Edge Minus</i>	92.01 \pm 0.94	90.29\pm0.88	97.87 \pm 0.15	97.16 \pm 0.97	98.14\pm0.66	95.50 \pm 0.43	97.90\pm0.29	89.47 \pm 1.86	85.39 \pm 1.08	96.05 \pm 0.37	97.97 \pm 0.31
	<i>Edge Mean</i>	91.86 \pm 0.76	89.61 \pm 0.96	97.94 \pm 0.13	97.19 \pm 1.00	98.08 \pm 0.66	95.52\pm0.43	97.70 \pm 0.36	89.62 \pm 1.82	85.23 \pm 1.00	96.08\pm0.35	98.07\pm0.27
	<i>Edge Att</i>	92.06\pm0.85	88.96 \pm 1.05	97.96\pm0.12	97.20\pm0.69	97.96 \pm 0.39	95.46 \pm 0.45	97.65 \pm 0.17	89.76\pm2.06	85.26 \pm 1.32	95.90 \pm 0.47	98.04 \pm 0.16
SAGE	<i>Original</i>	89.12 \pm 0.90	87.76 \pm 0.97	94.95 \pm 0.44	96.57 \pm 0.57	98.11 \pm 0.48	94.12 \pm 0.45	97.11 \pm 0.31	87.62 \pm 1.63	79.35 \pm 1.66	88.37 \pm 1.46	95.70 \pm 0.44
	<i>Edge Plus</i>	93.21 \pm 0.82	90.88 \pm 0.80	97.91 \pm 0.14	97.64 \pm 0.73	98.72\pm0.59	95.68 \pm 0.39	98.20 \pm 0.13	90.94\pm1.48	86.36 \pm 0.97	96.46\pm0.38	98.41 \pm 0.19
	<i>Edge Minus</i>	92.45 \pm 0.78	90.14 \pm 1.04	97.93 \pm 0.14	97.50 \pm 0.67	98.66 \pm 0.55	95.57 \pm 0.39	98.13 \pm 0.10	90.83 \pm 1.59	85.62 \pm 1.17	92.91 \pm 1.09	98.34 \pm 0.26
	<i>Edge Mean</i>	92.77 \pm 0.69	90.60 \pm 0.94	97.96 \pm 0.13	97.67\pm0.70	98.62 \pm 0.61	95.69\pm0.37	98.20 \pm 0.13	90.86 \pm 1.51	86.24 \pm 1.01	96.22 \pm 0.38	98.41 \pm 0.21
	<i>Edge Att</i>	93.31\pm1.02	91.01\pm1.14	98.01\pm0.13	97.40 \pm 0.94	98.70 \pm 0.59	95.49 \pm 0.49	98.22\pm0.24	90.64 \pm 1.88	86.46\pm0.91	96.31 \pm 0.59	98.43\pm0.13
GIN	<i>Original</i>	82.70 \pm 1.93	77.85 \pm 2.64	91.32 \pm 1.13	94.89 \pm 0.89	96.05 \pm 1.10	92.95 \pm 0.51	94.50 \pm 0.65	85.23 \pm 2.56	73.29 \pm 3.88	84.29 \pm 1.20	94.34 \pm 0.57
	<i>Edge Plus</i>	90.72 \pm 1.11	89.54 \pm 1.19	97.63\pm0.14	96.03 \pm 1.37	98.51 \pm 0.55	95.38 \pm 0.35	97.84\pm0.40	89.71\pm2.06	86.61\pm0.87	95.79\pm0.48	97.67 \pm 0.23
	<i>Edge Minus</i>	89.88 \pm 1.26	89.30 \pm 1.08	97.27 \pm 0.17	96.36 \pm 0.83	98.62 \pm 0.45	95.35 \pm 0.35	97.80 \pm 0.41	89.40 \pm 1.91	86.55 \pm 0.83	95.72 \pm 0.45	97.33 \pm 0.36
	<i>Edge Mean</i>	90.30 \pm 1.22	89.47 \pm 1.13	97.53 \pm 0.19	96.45\pm0.90	98.66\pm0.45	95.39\pm0.37	97.78 \pm 0.40	89.66 \pm 2.00	86.51 \pm 0.92	95.73 \pm 0.43	97.57 \pm 0.32
	<i>Edge Att</i>	90.76\pm0.88	89.55\pm0.61	97.50 \pm 0.15	96.34 \pm 0.82	98.35 \pm 0.54	95.29 \pm 0.29	97.66 \pm 0.33	89.39 \pm 1.61	86.21 \pm 0.92	96.31 \pm 0.52	97.74\pm0.33
PLNLP	<i>Original</i>	82.37 \pm 1.70	82.93 \pm 1.73	87.36 \pm 4.90	95.37 \pm 0.87	97.86 \pm 0.93	92.99 \pm 0.71	95.09 \pm 1.47	88.31 \pm 2.21	81.59 \pm 4.31	86.41 \pm 1.63	90.63 \pm 1.68
	<i>Edge Plus</i>	91.62 \pm 0.87	89.88\pm1.19	98.31 \pm 0.21	98.09 \pm 0.73	98.77\pm0.39	95.33\pm0.39	98.10 \pm 0.33	91.77\pm2.16	90.04 \pm 0.57	96.45\pm0.40	98.03\pm0.23
	<i>Edge Minus</i>	91.84\pm1.42	88.99 \pm 1.48	98.44\pm0.14	97.92 \pm 0.52	98.59 \pm 0.44	95.20 \pm 0.34	98.01 \pm 0.38	91.60 \pm 2.23	89.26 \pm 0.88	95.01 \pm 0.47	97.80 \pm 0.16
	<i>Edge Mean</i>	91.77 \pm 1.49	89.45 \pm 1.50	98.36 \pm 0.16	98.17\pm0.60	98.66 \pm 0.56	95.30 \pm 0.37	98.10\pm0.39	91.70 \pm 2.18	90.05 \pm 0.52	96.29 \pm 0.47	98.02 \pm 0.20
	<i>Edge Att</i>	91.22 \pm 1.34	88.75 \pm 1.70	98.41 \pm 0.17	98.13 \pm 0.61	98.70 \pm 0.40	95.32 \pm 0.38	98.06 \pm 0.37	91.72 \pm 2.12	90.08\pm0.54	96.40 \pm 0.40	98.01 \pm 0.18
SEAL	<i>Original</i>	90.13 \pm 1.94	87.59 \pm 1.57	95.79 \pm 0.78	97.26 \pm 0.58	97.44 \pm 1.07	95.06 \pm 0.46	96.91 \pm 0.45	88.75 \pm 1.90	78.14 \pm 3.14	92.35 \pm 1.21	97.33 \pm 0.28
	<i>Edge Plus</i>	90.01 \pm 1.95	89.65 \pm 1.22	97.30 \pm 0.34	97.34 \pm 0.59	98.35 \pm 0.63	95.35 \pm 0.38	97.67 \pm 0.32	89.20 \pm 1.86	85.25 \pm 0.80	95.47 \pm 0.58	97.84 \pm 0.25
	<i>Edge Minus</i>	91.04 \pm 1.91	89.74 \pm 1.16	97.50 \pm 0.33	97.27 \pm 0.63	98.17 \pm 0.74	95.36\pm0.37	97.64 \pm 0.30	89.35 \pm 1.98	85.30\pm0.91	95.77\pm0.79	97.79 \pm 0.30
	<i>Edge Mean</i>	90.36 \pm 1.17	89.87\pm1.14	97.52\pm0.34	97.38\pm0.68	98.23 \pm 0.70	95.30 \pm 0.34	97.68 \pm 0.33	89.19 \pm 1.85	85.30 \pm 0.87	95.61 \pm 0.64	97.83 \pm 0.23
	<i>Edge Att</i>	91.08\pm1.67	89.35 \pm 1.43	97.26 \pm 0.45	97.04 \pm 0.79	98.52\pm0.57	95.19 \pm 0.43	97.70\pm0.40	89.37\pm1.40	85.24 \pm 1.39	95.14 \pm 0.62	97.90\pm0.33
WalkPool	<i>Original</i>	92.00 \pm 0.79	89.64\pm1.01	97.70 \pm 0.19	97.83 \pm 0.97	99.00 \pm 0.45	94.53 \pm 0.44	96.81 \pm 0.92	93.71 \pm 1.11	82.43 \pm 3.57	87.46 \pm 7.45	95.00 \pm 0.90
	<i>Edge Plus</i>	91.96 \pm 0.79	89.49 \pm 0.96	98.36 \pm 0.13	97.97 \pm 0.96	98.99 \pm 0.58	95.47 \pm 0.32	98.28 \pm 0.24	93.79 \pm 1.11	91.24 \pm 0.84	97.31 \pm 0.26	98.65 \pm 0.17
	<i>Edge Minus</i>	91.97 \pm 0.80	89.61 \pm 1.04	98.43\pm0.10	98.03 \pm 0.95	99.02 \pm 0.54	95.47 \pm 0.32	98.30\pm0.23	93.83\pm1.13	91.28\pm0.90	97.35\pm0.28	98.66 \pm 0.17
	<i>Edge Mean</i>	91.77 \pm 0.74	89.55 \pm 1.09	98.39 \pm 0.11	98.01 \pm 0.89	99.02 \pm 0.56	95.47 \pm 0.29	98.30 \pm 0.24	93.70 \pm 1.12	91.26 \pm 0.81	97.27 \pm 0.29	98.65 \pm 0.19
	<i>Edge Att</i>	91.98 \pm 0.80	89.36 \pm 0.74	98.37 \pm 0.19	98.12\pm0.81	99.03\pm0.50	95.47\pm0.27	98.28 \pm 0.24	93.63 \pm 1.11	91.25 \pm 0.60	97.27 \pm 0.27	98.70\pm0.14

5.1 Experimental setup

Baseline methods. We show how FakeEdge techniques can improve the existing link prediction methods, including GAE-like models [10], PLNLP [14], SEAL [11], and WalkPool [12]. To examine the effectiveness of FakeEdge, we compare the model performance with subgraph representation learned on the **original** unmodified subgraph and the FakeEdge augmented ones. For GAE-like models, we apply different GNN encoders, including GCN [9], SAGE [43] and GIN [42]. SEAL and WalkPool have already been implemented in the fashion of the subgraph link prediction. However, a subgraph extraction preprocessing is needed for GAE and PLNLP, since they are not initially implemented as the subgraph link prediction. GCN, SAGE, and PLNLP use a score function to pool the subgraph. GCN and SAGE use the Hadamard product as the score function, while MLP is applied for PLNLP (see Section 3.2 for discussions about the score function). Moreover, GIN applies a subgraph-level pooling strategy, called "mean readout" [42], whose pooling is based on the entire subgraph. Similarly, SEAL and WalkPool also utilize the pooling on the entire subgraph to aggregate the representation. More details about the model implementation can be found in Appendix D.

Benchmark datasets. For the experiment, we use 3 datasets with node attributes and 8 without attributes. The graph datasets with node attributes are three citation networks: **Cora** [44], **Citeseer** [45], and **Pubmed** [46]. The graph datasets without node attributes are eight graphs in a variety of domains: **USAir** [47], **NS** [48], **PB** [49], **Yeast** [50], **C.ele** [51], **Power** [51], **Router** [52], and **E.coli** [53]. More details about the benchmark datasets can be found in Appendix E.

Evaluation protocols. Following the same experimental setting as of [11, 12], the links are split into 3 parts: 85% for training, 5% for validation, and 10% for testing. The links in validation and testing are unobserved during the training phase. We also implement a universal data pipeline for different methods to eliminate the data perturbation caused by train/test split. We perform 10 random data splits to reduce the performance disturbance. Area under the curve (AUC) [54] is used as the evaluation metrics and is reported by the epoch with the highest score on the validation set.

5.2 Results

FakeEdge on GAE-like models. The results of models with (*Edge Plus*, *Edge Minus*, *Edge Mean*, and *Edge Att*) and without (*Original*) FakeEdge are shown in Table 1. We observe that FakeEdge is a vital component for all different methods. With FakeEdge, the link prediction model can obtain a significant performance improvement on all datasets. GAE-like models and PLNLP achieve the most

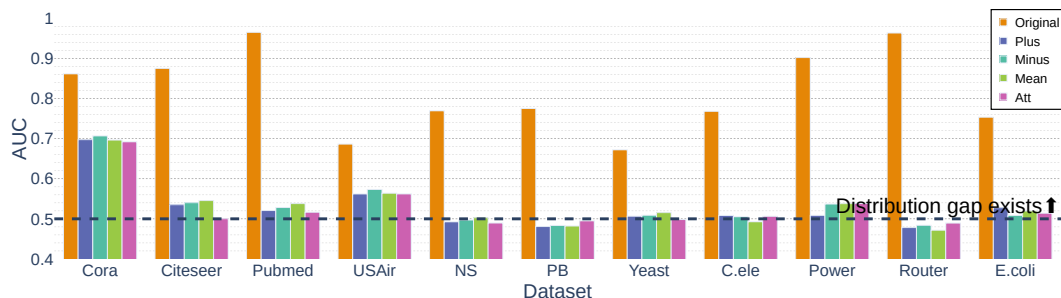


Figure 4: Distribution gap (AUC) of the positive samples between the training and testing set.

301 remarkable performance improvement when FakeEdge alleviates the dataset shift issue. FakeEdge
 302 boosts them by 2%-11% on different datasets. GCN, SAGE, and PLNLP all have a score function
 303 as the pooling methods, which is solely based on the focal node pair. In particular, the focal node
 304 pair is incident with the target link, which determines how the message passes around it. Therefore,
 305 the most severe dataset shift issues happen at the embedding of the focal node pair during the node
 306 representation learning step. FakeEdge is expected to bring a notable improvement to these situations.

307 **Encoder matters.** In addition, the choice of encoder plays an important role when GAE is deployed
 308 on the *Original* subgraph. We can see that SAGE shows the best performance without FakeEdge
 309 among these 3 encoders. However, after applying FakeEdge, all GAE-like methods achieve com-
 310 parable better results regardless of the choice of the encoder. We come to a hypothesis that the
 311 plain SAGE itself leverages the idea of FakeEdge to partially mitigate the dataset shift issue. Each
 312 node’s neighborhood in SAGE is a fixed-size set of nodes, which is uniformly sampled from the full
 313 neighborhood set. Thus, when learning the node representation of the focal node pair in the positive
 314 training sets, it is possible that one node of the focal node pair is not selected as the neighbor of
 315 the other node during the neighborhood sampling stage. In this case, the FakeEdge technique *Edge*
 316 *Minus* is applied to modify such a subgraph.

317 **FakeEdge on subgraph-based models.** In terms of SEAL and WalkPool, FakeEdge can still
 318 robustly enhance the model performance across different datasets. Especially for datasets like Power
 319 and Router, FakeEdge increases the AUC by over 10% on both methods. Both methods achieve better
 320 results across different datasets, except WalkPool model on datasets Cora and Citeseer. One of the
 321 crucial components of WalkPool is the walk-based pooling method, which actually operates on both
 322 the *Edge Plus* and *Edge Minus* graphs. Different from FakeEdge technique, WalkPool tackles the
 323 dataset shift problem mainly on the subgraph pooling stage. Thus, WalkPool shows similar model
 324 performance between the *Original* and FakeEdge augmented graphs. Moreover, SEAL and WalkPool
 325 have utilized one of the FakeEdge techniques as a trick in their initial implementations. However,
 326 they have failed to explicitly point out the fix of dataset shift issue from such a trick in their papers.

327 **Different FakeEdge techniques.** When comparing different FakeEdge techniques, *Edge Att* ap-
 328 pears to be the most stable, with a slightly better overall performance and a smaller variance. However,
 329 there is no significant difference between these techniques. This observation is consistent with our
 330 expectation since all FakeEdge techniques follow the same discipline to fix the dataset shift issue.

331 5.3 Further discussions

332 In this section, we conduct experiments to more thoroughly study why FakeEdge can improve the
 333 performance of the link prediction methods. We first give an empirical experiment to show how
 334 severe the distribution gap can be between training and testing. Then, we discuss the dataset shift
 335 issue with deeper GNNs.

336 5.3.1 Distribution gap between the training and testing

337 FakeEdge aims to produce Edge Invariant subgraph embedding during the training and testing phases
 338 in the link prediction task, especially for those positive samples $p(\mathbf{h}|y = 1)$. That is, the subgraph
 339 representation of the positive samples between the training and testing should be difficult, if at all,
 340 to be distinguishable from each other. Formally, we ask whether $p(\mathbf{h}|y = 1, c = \text{train}) = p(\mathbf{h}|y =$
 341 $1, c = \text{test})$, by conducting an empirical experiment on the subgraph embedding.

Table 2: GIN’s performance improvement by *Edge Att* compared to *Original* with a different number of layers. GIN utilizes mean-pooling as the subgraph-level readout.

Layers	Cora	Citeseer	Pubmed	USAir	NS	PB	Yeast	C.ele	Power	Router	E.coli
1	↑2.80%	↑3.65%	↑4.53%	↑0.29%	↑1.30%	↑1.02%	↑1.54%	↑2.13%	↑5.24%	↑11.19%	↑1.67%
2	↑4.66%	↑14.53%	↑6.64%	↑0.73%	↑1.55%	↑2.16%	↑3.40%	↑5.41%	↑25.32%	↑14.73%	↑2.59%
3	↑9.78%	↑15.19%	↑6.57%	↑0.98%	↑2.49%	↑2.43%	↑3.60%	↑4.48%	↑20.46%	↑13.38%	↑3.14%

We retrieve the subgraph embedding of the positive samples from both the training and testing stages, and randomly shuffle the embedding. Then we classify whether the sample is from training ($c = \text{train}$) or testing ($c = \text{test}$). The shuffled positive samples are split 80%/20% as train and inference sets. Note that the train set here, as well as the inference set, contains both the shuffled positive samples from the training and testing set in the link prediction task. Then we feed the subgraph embedding into a 2-layer MLP classifier to investigate whether the classifier can differentiate the training samples ($c = \text{train}$) and the testing samples ($c = \text{test}$). In general, the classifier will struggle to undertake the classification if the embedding of training and testing samples is drawn from the same underlying distribution, which indicates there is no significant dataset shift issue.

We use GAE with the GCN as the encoder to run the experiment. AUC is used to measure the discriminating power of the classifier. The results are shown in Figure 4. Without FakeEdge, the classifier shows a significant ability to separate positive samples between training and testing. When it comes to the subgraph embedding with FakeEdge, the classifier stumbles in distinguishing the samples. The comparison clearly reveals how different the subgraph embedding can be between the training and testing, while FakeEdge can both provably and empirically diminish the distribution gap.

5.3.2 Dataset shift with deeper GNNs

Given two graphs with n nodes in each graph, 1-WL test may take up to n iterations to determine whether two graphs are isomorphic [55]. Thus, GNNs, which mimic 1-WL test, tend to discriminate more non-isomorphic graphs when the number of GNN layers increases. SEAL [19] has empirically witnessed a stronger representation power and obtained more expressive link representation with deeper GNNs. However, we notice that the dataset shift issue in the subgraph link prediction becomes more severe when GNNs try to capture long-range information with more layers.

We reproduce the experiments on GIN by using $l = 1, 2, 3$ message passing layers and compare the model performance by AUC scores with and without FakeEdge. Here we only apply *Edge Att* as the FakeEdge technique. The relative AUC score improvement of *Edge Att* is reported, namely $(AUC_{EdgeAtt} - AUC_{Original}) / AUC_{Original}$. The results are shown in Table 2. As we can observe, the relative performance improvement between *Edge Att* and *Original* becomes more significant with more layers, which indicates that the dataset shift issue can be potentially more critical when we seek deeper GNNs for greater predictive power.

To explain such a phenomenon, we hypothesize that GNNs with more layers will involve more nodes in the subgraph, such that their computation graph is dependent on the existence of the edge at the focal node pair. For example, select a node v from the subgraph $\mathcal{G}_{i,j}^r$, which is at least l hops away from the focal node pair $\{i, j\}$, namely $l = \min(d(i, v), d(j, v))$. If the GNN has only l layers, v will not include the edge (i, j) in its computation graph. But with a GNN with $l + 1$ layers, the edge (i, j) will affect v ’s computation graph. We leave the validation of the hypothesis to future work.

6 Conclusion

Dataset shift is arguably one of the most challenging problems in the world of machine learning. However, to the best of our knowledge, none of the previous studies sheds light on this notable phenomenon in link prediction. In this paper, we studied the issue of dataset shift in link prediction tasks with GNN-based models. We first unified several existing models into a framework of subgraph link prediction. Then, we theoretically investigated the phenomenon of dataset shift in subgraph link prediction and proposed a model-agnostic technique FakeEdge to amend the issue. Experiments with different models over a wide range of datasets verified the effectiveness of FakeEdge.

References

- 385
- 386 [1] David Liben-Nowell and Jon Kleinberg. The link prediction problem for social networks. In
 387 *Proceedings of the twelfth international conference on Information and knowledge management*,
 388 CIKM '03, pages 556–559, New York, NY, USA, November 2003. Association for Computing
 389 Machinery. ISBN 978-1-58113-723-1. doi: 10.1145/956863.956972. URL [http://doi.org/](http://doi.org/10.1145/956863.956972)
 390 [10.1145/956863.956972](http://doi.org/10.1145/956863.956972). 1, 2, 4, 14, 17
- 391 [2] Damian Szklarczyk, Annika L. Gable, David Lyon, Alexander Junge, Stefan Wyder, Jaime
 392 Huerta-Cepas, Milan Simonovic, Nadezhda T. Doncheva, John H. Morris, Peer Bork, Lars J.
 393 Jensen, and Christian von Mering. STRING v11: protein-protein association networks with
 394 increased coverage, supporting functional discovery in genome-wide experimental datasets.
 395 *Nucleic Acids Research*, 47(D1):D607–D613, January 2019. ISSN 1362-4962. doi: 10.1093/
 396 nar/gky1131. 1
- 397 [3] Yehuda Koren, Robert Bell, and Chris Volinsky. Matrix factorization techniques for recom-
 398 mender systems. *Computer*, 42(8):30–37, 2009. Publisher: IEEE. 1
- 399 [4] Zhilin Yang, William Cohen, and Ruslan Salakhudinov. Revisiting semi-supervised learning
 400 with graph embeddings. In *International conference on machine learning*, pages 40–48. PMLR,
 401 2016. 1
- 402 [5] Yang Yang, Ryan N. Lichtenwalter, and Nitesh V. Chawla. Evaluating link prediction methods.
 403 *Knowledge and Information Systems*, 45(3):751–782, December 2015. ISSN 0219-3116. doi:
 404 [10.1007/s10115-014-0789-0](https://doi.org/10.1007/s10115-014-0789-0). URL <https://doi.org/10.1007/s10115-014-0789-0>. 1
- 405 [6] Michaël Defferrard, Xavier Bresson, and Pierre Vandergheynst. Convolutional Neural Networks
 406 on Graphs with Fast Localized Spectral Filtering. In D. Lee, M. Sugiyama, U. Luxburg, I. Guyon,
 407 and R. Garnett, editors, *Advances in Neural Information Processing Systems*, volume 29.
 408 Curran Associates, Inc., 2016. URL [https://proceedings.neurips.cc/paper/2016/](https://proceedings.neurips.cc/paper/2016/file/04df4d434d481c5bb723be1b6df1ee65-Paper.pdf)
 409 [file/04df4d434d481c5bb723be1b6df1ee65-Paper.pdf](https://proceedings.neurips.cc/paper/2016/file/04df4d434d481c5bb723be1b6df1ee65-Paper.pdf). 1
- 410 [7] David K Duvenaud, Dougal Maclaurin, Jorge Iparraguirre, Rafael Bombarell, Timothy
 411 Hirzel, Alan Aspuru-Guzik, and Ryan P Adams. Convolutional Networks on Graphs for
 412 Learning Molecular Fingerprints. In C. Cortes, N. Lawrence, D. Lee, M. Sugiyama, and
 413 R. Garnett, editors, *Advances in Neural Information Processing Systems*, volume 28. Cur-
 414 ran Associates, Inc., 2015. URL [https://proceedings.neurips.cc/paper/2015/file/](https://proceedings.neurips.cc/paper/2015/file/f9be311e65d81a9ad8150a60844bb94c-Paper.pdf)
 415 [f9be311e65d81a9ad8150a60844bb94c-Paper.pdf](https://proceedings.neurips.cc/paper/2015/file/f9be311e65d81a9ad8150a60844bb94c-Paper.pdf).
- 416 [8] Joan Bruna, Wojciech Zaremba, Arthur Szlam, and Yann LeCun. Spectral Networks and
 417 Locally Connected Networks on Graphs. *arXiv:1312.6203 [cs]*, May 2014. URL [http:](http://arxiv.org/abs/1312.6203)
 418 [//arxiv.org/abs/1312.6203](http://arxiv.org/abs/1312.6203). arXiv: 1312.6203.
- 419 [9] Thomas N. Kipf and Max Welling. Semi-Supervised Classification with Graph Convolutional
 420 Networks. *arXiv:1609.02907 [cs, stat]*, February 2017. URL [http://arxiv.org/abs/1609.](http://arxiv.org/abs/1609.02907)
 421 [02907](http://arxiv.org/abs/1609.02907). arXiv: 1609.02907. 1, 7, 14, 15
- 422 [10] Thomas N. Kipf and Max Welling. Variational Graph Auto-Encoders, 2016. *_eprint:*
 423 [1611.07308](https://arxiv.org/abs/1611.07308). 1, 4, 7, 14
- 424 [11] Muhan Zhang and Yixin Chen. Link Prediction Based on Graph Neural Networks.
 425 In S. Bengio, H. Wallach, H. Larochelle, K. Grauman, N. Cesa-Bianchi, and R. Gar-
 426 nett, editors, *Advances in Neural Information Processing Systems*, volume 31. Curran
 427 Associates, Inc., 2018. URL [https://proceedings.neurips.cc/paper/2018/file/](https://proceedings.neurips.cc/paper/2018/file/53f0d7c537d99b3824f0f99d62ea2428-Paper.pdf)
 428 [53f0d7c537d99b3824f0f99d62ea2428-Paper.pdf](https://proceedings.neurips.cc/paper/2018/file/53f0d7c537d99b3824f0f99d62ea2428-Paper.pdf). 1, 2, 4, 7, 14, 15
- 429 [12] Liming Pan, Cheng Shi, and Ivan Dokmanić. Neural Link Prediction with Walk Pooling. In
 430 *International Conference on Learning Representations*, 2022. URL [https://openreview.](https://openreview.net/forum?id=CCu6RcUMwKO)
 431 [net/forum?id=CCu6RcUMwKO](https://openreview.net/forum?id=CCu6RcUMwKO). 2, 4, 7, 14, 15
- 432 [13] Pan Li, Yanbang Wang, Hongwei Wang, and Jure Leskovec. Distance Encoding: De-
 433 sign Provably More Powerful Neural Networks for Graph Representation Learning. In
 434 H. Larochelle, M. Ranzato, R. Hadsell, M. F. Balcan, and H. Lin, editors, *Advances*
 435 *in Neural Information Processing Systems*, volume 33, pages 4465–4478. Curran As-
 436 sociates, Inc., 2020. URL [https://proceedings.neurips.cc/paper/2020/file/](https://proceedings.neurips.cc/paper/2020/file/2f73168bf3656f697507752ec592c437-Paper.pdf)
 437 [2f73168bf3656f697507752ec592c437-Paper.pdf](https://proceedings.neurips.cc/paper/2020/file/2f73168bf3656f697507752ec592c437-Paper.pdf). 14

- 438 [14] Zhitao Wang, Yong Zhou, Litao Hong, Yuanhang Zou, Hanjing Su, and Shouzhi Chen. Pairwise
439 Learning for Neural Link Prediction. *arXiv:2112.02936 [cs]*, January 2022. URL [http://
440 //arxiv.org/abs/2112.02936](http://arxiv.org/abs/2112.02936). arXiv: 2112.02936. 1, 4, 7, 14, 15
- 441 [15] Joaquin Quiñero-Candela, Masashi Sugiyama, Anton Schwaighofer, Neil D. Lawrence,
442 Michael I. Jordan, and Thomas G. Dietterich, editors. *Dataset Shift in Machine Learning*.
443 Neural Information Processing series. MIT Press, Cambridge, MA, USA, December 2008.
444 ISBN 978-0-262-17005-5. 1
- 445 [16] Jose G. Moreno-Torres, Troy Raeder, Rocío Alaiz-Rodríguez, Nitesh V. Chawla, and Francisco
446 Herrera. A unifying view on dataset shift in classification. *Pattern Recognition*, 45(1):521–530,
447 January 2012. ISSN 0031-3203. doi: 10.1016/j.patcog.2011.06.019. URL [http://doi.org/
448 10.1016/j.patcog.2011.06.019](http://doi.org/10.1016/j.patcog.2011.06.019). 1, 2
- 449 [17] Justin Gilmer, Samuel S. Schoenholz, Patrick F. Riley, Oriol Vinyals, and George E. Dahl.
450 Neural Message Passing for Quantum Chemistry. *CoRR*, abs/1704.01212, 2017. URL [http://
451 //arxiv.org/abs/1704.01212](http://arxiv.org/abs/1704.01212). arXiv: 1704.01212. 1, 5, 14
- 452 [18] Boris Weisfeiler and Andrei Leman. The reduction of a graph to canonical form and the algebra
453 which appears therein. *NTI, Series*, 2(9):12–16, 1968. 1
- 454 [19] Muhan Zhang, Pan Li, Yinglong Xia, Kai Wang, and Long Jin. Labeling Trick: A The-
455 ory of Using Graph Neural Networks for Multi-Node Representation Learning. In M. Ran-
456 zato, A. Beygelzimer, Y. Dauphin, P. S. Liang, and J. Wortman Vaughan, editors, *Ad-
457 vances in Neural Information Processing Systems*, volume 34, pages 9061–9073. Curran
458 Associates, Inc., 2021. URL [https://proceedings.neurips.cc/paper/2021/file/
459 4be49c79f233b4f4070794825c323733-Paper.pdf](https://proceedings.neurips.cc/paper/2021/file/4be49c79f233b4f4070794825c323733-Paper.pdf). 2, 6, 9, 15
- 460 [20] Lada A. Adamic and Eytan Adar. Friends and neighbors on the Web. *Social Networks*, 25(3):
461 211–230, 2003. ISSN 0378-8733. doi: [https://doi.org/10.1016/S0378-8733\(03\)00009-1](https://doi.org/10.1016/S0378-8733(03)00009-1). URL
462 <https://www.sciencedirect.com/science/article/pii/S0378873303000091>. 2, 4,
463 14, 17
- 464 [21] Gilad Yehudai, Ethan Fetaya, Eli Meir, Gal Chechik, and Haggai Maron. From Local
465 Structures to Size Generalization in Graph Neural Networks, July 2021. URL [http://arxiv.
466 org/abs/2010.08853](http://arxiv.org/abs/2010.08853). arXiv:2010.08853 [cs, stat]. 2
- 467 [22] Qi Zhu, Natalia Ponomareva, Jiawei Han, and Bryan Perozzi. Shift-Robust GNNs:
468 Overcoming the Limitations of Localized Graph Training data. In M. Ranzato,
469 A. Beygelzimer, Y. Dauphin, P. S. Liang, and J. Wortman Vaughan, editors, *Advances
470 in Neural Information Processing Systems*, volume 34, pages 27965–27977. Curran As-
471 sociates, Inc., 2021. URL [https://proceedings.neurips.cc/paper/2021/file/
472 eb55e369affa90f77dd7dc9e2cd33b16-Paper.pdf](https://proceedings.neurips.cc/paper/2021/file/eb55e369affa90f77dd7dc9e2cd33b16-Paper.pdf). 2
- 473 [23] Qitian Wu, Hengrui Zhang, Junchi Yan, and David Wipf. Handling Distribution Shifts on
474 Graphs: An Invariance Perspective. May 2022. URL [https://openreview.net/forum?
475 id=FQ0C5u-1egI](https://openreview.net/forum?id=FQ0C5u-1egI). 2
- 476 [24] Yangze Zhou, Gitta Kutyniok, and Bruno Ribeiro. OOD Link Prediction Generalization
477 Capabilities of Message-Passing GNNs in Larger Test Graphs, 2022. URL [https://arxiv.
478 org/abs/2205.15117](https://arxiv.org/abs/2205.15117). 3
- 479 [25] Beatrice Bevilacqua, Yangze Zhou, and Bruno Ribeiro. Size-Invariant Graph Representations
480 for Graph Classification Extrapolations, 2021. URL <https://arxiv.org/abs/2103.05045>.
481 3
- 482 [26] Davide Buffelli, Pietro Liò, and Fabio Vandin. SizeShiftReg: a Regularization Method for
483 Improving Size-Generalization in Graph Neural Networks, 2022. URL [https://arxiv.org/
484 abs/2207.07888](https://arxiv.org/abs/2207.07888).
- 485 [27] Sohir Maskey, Ron Levie, Yunseok Lee, and Gitta Kutyniok. Generalization Analysis of
486 Message Passing Neural Networks on Large Random Graphs, 2022. URL [https://arxiv.
487 org/abs/2202.00645](https://arxiv.org/abs/2202.00645). 3
- 488 [28] Tong Zhao, Gang Liu, Stephan Günnemann, and Meng Jiang. Graph Data Augmentation for
489 Graph Machine Learning: A Survey. *arXiv e-prints*, page arXiv:2202.08871, February 2022.
490 _eprint: 2202.08871. 3

- 491 [29] Yu Rong, Wenbing Huang, Tingyang Xu, and Junzhou Huang. DropEdge: Towards Deep Graph
492 Convolutional Networks on Node Classification. In *International Conference on Learning*
493 *Representations*, 2020. URL <https://openreview.net/forum?id=Hkx1qkrKPr>. 3
- 494 [30] Deli Chen, Yankai Lin, Wei Li, Peng Li, Jie Zhou, and Xu Sun. Measuring and Relieving the
495 Over-smoothing Problem for Graph Neural Networks from the Topological View. In *AAAI*,
496 2020. 3
- 497 [31] Jake Topping, Francesco Di Giovanni, Benjamin Paul Chamberlain, Xiaowen Dong, and
498 Michael M. Bronstein. Understanding over-squashing and bottlenecks on graphs via curvature.
499 *arXiv:2111.14522 [cs, stat]*, November 2021. URL <http://arxiv.org/abs/2111.14522>.
500 arXiv: 2111.14522. 3
- 501 [32] Uri Alon and Eran Yahav. On the Bottleneck of Graph Neural Networks and its Practical
502 Implications. *arXiv:2006.05205 [cs, stat]*, March 2021. URL [http://arxiv.org/abs/2006.](http://arxiv.org/abs/2006.05205)
503 [05205](http://arxiv.org/abs/2006.05205). arXiv: 2006.05205. 3
- 504 [33] Johannes Klicpera, Stefan Weissenberger, and Stephan Günnemann. Diffusion Improves Graph
505 Learning. *arXiv:1911.05485 [cs, stat]*, December 2019. URL [http://arxiv.org/abs/1911.](http://arxiv.org/abs/1911.05485)
506 [05485](http://arxiv.org/abs/1911.05485). arXiv: 1911.05485. 3
- 507 [34] Tong Zhao, Gang Liu, Daheng Wang, Wenhao Yu, and Meng Jiang. Learning from Counterfac-
508 tual Links for Link Prediction. In Kamalika Chaudhuri, Stefanie Jegelka, Le Song, Csaba Szepes-
509 vari, Gang Niu, and Sivan Sabato, editors, *Proceedings of the 39th International Conference on*
510 *Machine Learning*, volume 162 of *Proceedings of Machine Learning Research*, pages 26911–
511 26926. PMLR, July 2022. URL <https://proceedings.mlr.press/v162/zhao22e.html>.
512 3
- 513 [35] Abhay Singh, Qian Huang, Sijia Linda Huang, Omkar Bhalerao, Horace He, Ser-Nam Lim, and
514 Austin R. Benson. Edge Proposal Sets for Link Prediction. Technical Report arXiv:2106.15810,
515 arXiv, June 2021. URL <http://arxiv.org/abs/2106.15810>. arXiv:2106.15810 [cs] type:
516 article. 3
- 517 [36] Muhan Zhang, Zhicheng Cui, Marion Neumann, and Yixin Chen. An End-to-End Deep
518 Learning Architecture for Graph Classification. *Proceedings of the AAAI Conference on*
519 *Artificial Intelligence*, 32(1), April 2018. ISSN 2374-3468. doi: 10.1609/aaai.v32i1.11782.
520 URL <https://ojs.aaai.org/index.php/AAAI/article/view/11782>. Number: 1. 4
- 521 [37] Albert-László Barabási and Réka Albert. Emergence of Scaling in Random Net-
522 works. *Science*, 286(5439):509–512, 1999. doi: 10.1126/science.286.5439.509.
523 URL <https://www.science.org/doi/abs/10.1126/science.286.5439.509>. _eprint:
524 <https://www.science.org/doi/pdf/10.1126/science.286.5439.509>. 4, 14, 17
- 525 [38] Paul Jaccard. The Distribution of the Flora in the Alpine Zone.1. *New Phytologist*, 11(2):
526 37–50, 1912. ISSN 1469-8137. doi: 10.1111/j.1469-8137.1912.tb05611.x. URL <https://onlinelibrary.wiley.com/doi/abs/10.1111/j.1469-8137.1912.tb05611.x>.
527 _eprint: <https://onlinelibrary.wiley.com/doi/pdf/10.1111/j.1469-8137.1912.tb05611.x>. 4, 17
- 528 [39] Tao Zhou, Linyuan Lü, and Yi-Cheng Zhang. Predicting missing links via local information.
529 *The European Physical Journal B*, 71(4):623–630, 2009. Publisher: Springer. 4, 17
- 530 [40] Minh-Thang Luong, Hieu Pham, and Christopher D. Manning. Effective Approaches to
531 Attention-based Neural Machine Translation, 2015. URL [https://arxiv.org/abs/1508.](https://arxiv.org/abs/1508.04025)
532 [04025](https://arxiv.org/abs/1508.04025). 6
- 533 [41] Balasubramaniam Srinivasan and Bruno Ribeiro. On the Equivalence between Positional Node
534 Embeddings and Structural Graph Representations. In *International Conference on Learning*
535 *Representations*, 2020. URL <https://openreview.net/forum?id=SJxzFySKwH>. 6
- 536 [42] Keyulu Xu, Weihua Hu, Jure Leskovec, and Stefanie Jegelka. How Powerful are Graph Neural
537 Networks? *CoRR*, abs/1810.00826, 2018. URL <http://arxiv.org/abs/1810.00826>.
538 arXiv: 1810.00826. 6, 7, 15
- 539 [43] William L. Hamilton, Rex Ying, and Jure Leskovec. Inductive Representation Learning on
540 Large Graphs. *arXiv:1706.02216 [cs, stat]*, September 2018. URL [http://arxiv.org/abs/](http://arxiv.org/abs/1706.02216)
541 [1706.02216](http://arxiv.org/abs/1706.02216). arXiv: 1706.02216. 7, 15
- 542 [44] Andrew Kachites McCallum, Kamal Nigam, Jason Rennie, and Kristie Seymore. Automating
543 the construction of internet portals with machine learning. *Information Retrieval*, 3(2):127–163,
544 2000. Publisher: Springer. 7, 15
- 545

- 546 [45] C Lee Giles, Kurt D Bollacker, and Steve Lawrence. CiteSeer: An automatic citation indexing
547 system. In *Proceedings of the third ACM conference on Digital libraries*, pages 89–98, 1998. 7,
548 15
- 549 [46] Galileo Namata, Ben London, Lise Getoor, and Bert Huang. Query-driven active surveying for
550 collective classification. In *10th International Workshop on Mining and Learning with Graphs*,
551 volume 8, page 1, 2012. 7, 15
- 552 [47] Vladimir Batagelj and Andrej Mrvar. Pajek datasets website, 2006. URL [http://vlado.fmf.
553 uni-lj.si/pub/networks/data/](http://vlado.fmf.uni-lj.si/pub/networks/data/). 7, 15
- 554 [48] Mark EJ Newman. Finding community structure in networks using the eigenvectors of matrices.
555 *Physical review E*, 74(3):036104, 2006. Publisher: APS. 7, 15
- 556 [49] Robert Ackland and others. Mapping the US political blogosphere: Are conservative bloggers
557 more prominent? In *BlogTalk Downunder 2005 Conference, Sydney*, 2005. 7, 15
- 558 [50] Christian Von Mering, Roland Krause, Berend Snel, Michael Cornell, Stephen G Oliver, Stanley
559 Fields, and Peer Bork. Comparative assessment of large-scale data sets of protein–protein
560 interactions. *Nature*, 417(6887):399–403, 2002. Publisher: Nature Publishing Group. 7, 15
- 561 [51] Duncan J Watts and Steven H Strogatz. Collective dynamics of ‘small-world’ networks. *nature*,
562 393(6684):440–442, 1998. Publisher: Nature Publishing Group. 7, 15
- 563 [52] Neil Spring, Ratul Mahajan, and David Wetherall. Measuring ISP topologies with Rocketfuel.
564 *ACM SIGCOMM Computer Communication Review*, 32(4):133–145, 2002. Publisher: ACM
565 New York, NY, USA. 7, 15
- 566 [53] Muhan Zhang, Zhicheng Cui, Shali Jiang, and Yixin Chen. Beyond link prediction: Predicting
567 hyperlinks in adjacency space. In *Thirty-Second AAAI Conference on Artificial Intelligence*,
568 2018. 7, 15
- 569 [54] Andrew P. Bradley. The use of the area under the ROC curve in the evaluation of machine
570 learning algorithms. *Pattern Recognition*, 30(7):1145–1159, July 1997. ISSN 0031-3203.
571 doi: 10.1016/S0031-3203(96)00142-2. URL [https://www.sciencedirect.com/science/
572 article/pii/S0031320396001422](https://www.sciencedirect.com/science/article/pii/S0031320396001422). 7
- 573 [55] Nino Shervashidze, Pascal Schweitzer, Erik Jan Van Leeuwen, Kurt Mehlhorn, and Karsten M
574 Borgwardt. Weisfeiler-lehman graph kernels. *Journal of Machine Learning Research*, 12(9),
575 2011. 9
- 576 [56] Muhan Zhang and Yixin Chen. Weisfeiler-Lehman Neural Machine for Link Prediction. In
577 *Proceedings of the 23rd ACM SIGKDD International Conference on Knowledge Discovery and
578 Data Mining*, pages 575–583, Halifax NS Canada, August 2017. ACM. ISBN 978-1-4503-4887-
579 4. doi: 10.1145/3097983.3097996. URL [https://dl.acm.org/doi/10.1145/3097983.
580 3097996](https://dl.acm.org/doi/10.1145/3097983.3097996). 14
- 581 [57] Ron Milo, Shalev Itzkovitz, Nadav Kashtan, Reuven Levitt, Shai Shen-Orr, In-
582 bal Ayzenshtat, Michal Sheffer, and Uri Alon. Superfamilies of Evolved and De-
583 signed Networks. *Science*, 303(5663):1538–1542, 2004. doi: 10.1126/science.
584 1089167. URL [https://www.science.org/doi/abs/10.1126/science.1089167.
585 _eprint: https://www.science.org/doi/pdf/10.1126/science.1089167](https://www.science.org/doi/abs/10.1126/science.1089167). 14
- 586 [58] Yang Hu, Xiyuan Wang, Zhouchen Lin, Pan Li, and Muhan Zhang. Two-Dimensional Weisfeiler-
587 Lehman Graph Neural Networks for Link Prediction, June 2022. URL [http://arxiv.org/
588 abs/2206.09567](http://arxiv.org/abs/2206.09567). arXiv:2206.09567 [cs]. 14
- 589 [59] Weihua Hu, Matthias Fey, Marinka Zitnik, Yuxiao Dong, Hongyu Ren, Bowen Liu, Michele
590 Catasta, and Jure Leskovec. Open Graph Benchmark: Datasets for Machine Learning on Graphs.
591 *arXiv:2005.00687 [cs, stat]*, February 2021. URL <http://arxiv.org/abs/2005.00687>.
592 arXiv: 2005.00687. 16
- 593 [60] Xiyuan Wang and Muhan Zhang. How Powerful are Spectral Graph Neural Networks. In
594 Kamalika Chaudhuri, Stefanie Jegelka, Le Song, Csaba Szepesvari, Gang Niu, and Sivan Sabato,
595 editors, *Proceedings of the 39th International Conference on Machine Learning*, volume 162
596 of *Proceedings of Machine Learning Research*, pages 23341–23362. PMLR, July 2022. URL
597 <https://proceedings.mlr.press/v162/wang22am.html>. 18

598 A Related work of link predictions

599 Early studies on link prediction problems mainly focus on heuristics methods, which require expertise on the underlying trait of network or hand-crafted features, including Common Neighbor [1],
 600 Adamic–Adar index [20] and Preferential Attachment [37], etc. WLNLM [56] suggests a method to
 601 encode the induced subgraph of the target link as an adjacency matrix to represent the link. With the
 602 huge success of GNN [9], GNN-based link prediction methods have become dominant across different
 603 areas. Graph Auto Encoder(GAE) and Variational Graph Auto Encoder(VGAE) [10] perform link
 604 prediction tasks by reconstructing the graph structure. SEAL [11] and DE [13] propose methods
 605 to label the nodes according to the distance to the focal node pair. To better exploit the structural
 606 motifs [57] in distinct graphs, a walk-based pooling method (WalkPool) [12] is designed to extract
 607 the representation of the local neighborhood. PLNLP [14] sheds light on pairwise learning to rank
 608 the node pairs of interest. Based on two-dimensional Weisfeiler-Lehman tests, Hu et al. propose a
 609 link prediction method that can directly obtain node pair representation [58].

611 B Proof of Theorem 1

612 We restate the [Theorem 1](#): GNN cannot learn the subgraph feature \mathbf{h} to be Edge Invariant.

613 *Proof.* Recall that the computation of subgraph feature \mathbf{h} involves steps such as:

- 614 1. **Subgraph Extraction:** Extract the subgraph $\mathcal{G}_{i,j}^r$ around the focal node pair $\{i, j\}$;
- 615 2. **Node Representation Learning:** $\mathbf{Z} = \text{GNN}(\mathcal{G}_{i,j}^r)$, where $\mathbf{Z} \in \mathbb{R}^{|\mathcal{V}_{i,j}^r| \times F_{\text{hidden}}}$ is the node embed-
 616 ding matrix learned by the GNN encoder;
- 617 3. **Pooling:** $\mathbf{h} = \text{Pooling}(\mathbf{Z}; \mathcal{G}_{i,j}^r)$, where $\mathbf{h} \in \mathbb{R}^{F_{\text{pooled}}}$ is the latent feature of the subgraph $\mathcal{G}_{i,j}^r$;

618 Here, GNN is Message Passing Neural Network [17]. Given a subgraph $\mathcal{G} = (V, E, \mathbf{x}^V, \mathbf{x}^E)$, GNN
 619 with T layers applies following rules to update the representation of node $i \in V$:

$$h_i^{(t+1)} = U_t(h_i^{(t)}, \sum_{w \in \mathcal{N}(i)} M_t(h_i^{(t)}, h_w^{(t)}, \mathbf{x}_{i,w}^E)), \quad (3)$$

620 where $\mathcal{N}(i)$ is the neighborhood of node i in \mathcal{G} , M_t is the message passing function at layer t and U_t
 621 is the node update function at layer t . The hidden states at the first layer are set as $h_i^{(0)} = \mathbf{x}_i^V$. The
 622 hidden states at the last layer are the outputs $\mathbf{Z}_i = h_i^{(T)}$.

623 Given any subgraph $\mathcal{G}_{i,j}^r = (V_{i,j}^r, E_{i,j}^r, \mathbf{x}_{V_{i,j}^r}^V, \mathbf{x}_{E_{i,j}^r}^E)$ with the edge present at the focal node pair
 624 $(i, j) \in E_{i,j}^r$, we construct another isomorphic subgraph $\mathcal{G}_{\bar{i},\bar{j}}^r = (V_{\bar{i},\bar{j}}^r, E_{\bar{i},\bar{j}}^r, \mathbf{x}_{V_{\bar{i},\bar{j}}^r}^V, \mathbf{x}_{E_{\bar{i},\bar{j}}^r}^E)$, but remove
 625 the edge (\bar{i}, \bar{j}) from the edge set $E_{\bar{i},\bar{j}}^r$ of the subgraph. $\mathcal{G}_{\bar{i},\bar{j}}^r$ can be seen as the counterpart of $\mathcal{G}_{i,j}^r$ in
 626 the testing set.

627 Thus, for the first iteration of node updates $t = 1$:

$$h_i^{(1)} = U_t(h_i^{(0)}, \sum_{w \in \mathcal{N}(i)} M_t(h_i^{(0)}, h_w^{(0)}, \mathbf{x}_{i,w}^E)), \quad (4)$$

$$h_{\bar{i}}^{(1)} = U_t(h_{\bar{i}}^{(0)}, \sum_{w \in \mathcal{N}(\bar{i})} M_t(h_{\bar{i}}^{(0)}, h_w^{(0)}, \mathbf{x}_{\bar{i},w}^E)), \quad (5)$$

628 Note that $\mathcal{N}(\bar{i}) \cup \{j\} = \mathcal{N}(i)$. We have:

$$h_i^{(1)} = U_t(h_i^{(0)}, \sum_{w \in \mathcal{N}(i) \setminus \{j\}} M_t(h_i^{(0)}, h_w^{(0)}, \mathbf{x}_{i,w}^E) + M_t(h_i^{(0)}, h_j^{(0)}, \mathbf{x}_{i,j}^E)) \quad (6)$$

$$= U_t(h_i^{(0)}, \sum_{w \in \mathcal{N}(\bar{i})} M_t(h_i^{(0)}, h_w^{(0)}, \mathbf{x}_{i,w}^E) + M_t(h_i^{(0)}, h_j^{(0)}, \mathbf{x}_{i,\bar{j}}^E)), \quad (7)$$

629 As U_t is injective, $p(h_i^{(1)}, y = 1 | e = 1) \neq p(h_{\bar{i}}^{(1)}, y = 1) = p(h_i^{(1)}, y = 1 | e = 0)$. Similarly, we can
 630 conclude that $p(h_i^{(T)}, y = 1 | e = 1) \neq p(h_{\bar{i}}^{(T)}, y = 1 | e = 0)$.

631 As we use the last iteration of node updates $h_i^{(T)}$ as the final node representation \mathbf{Z} , we have
 632 $p(\mathbf{Z}, y|e = 1) \neq p(\mathbf{Z}, y|e = 0)$, which leads to $p(\mathbf{h}, y|e = 1) \neq p(\mathbf{h}, y|e = 0)$ and concludes the
 633 proof. \square

634 C Proof of Theorem 2

635 We restate the **Theorem 2**: Given $p(\mathbf{h}, y|e, c) = p(\mathbf{h}, y|e)$, there is no **Dataset Shift** in the link pre-
 636 diction if the subgraph embedding is **Edge Invariant**. That is, $p(\mathbf{h}, y|e) = p(\mathbf{h}, y) \implies p(\mathbf{h}, y|c) =$
 637 $p(\mathbf{h}, y)$.

Proof.

$$p(\mathbf{h} = \mathbf{h}, y = y|c = c) \tag{8}$$

$$= \mathbb{E}_e[p(\mathbf{h} = \mathbf{h}, y = y|c = c, e)p(e|c = c)] \tag{9}$$

$$= \mathbb{E}_e[p(\mathbf{h} = \mathbf{h}, y = y)p(e|c = c)] \tag{10}$$

$$= p(\mathbf{h} = \mathbf{h}, y = y). \tag{11}$$

638 \square

639 D Details about the baseline methods

640 To verify the effectiveness of FakeEdge, we tend to introduce minimal modification to the baseline
 641 models and make them compatible with FakeEdge techniques. The baseline models in our experiments
 642 are mainly from the two streams of link prediction models. One is the GAE-like model, including
 643 GCN [9], SAGE [43], GIN [42] and PLNLP [14]. The other includes SEAL [11] and WalkPool [12].
 644 GCN, SAGE and PLNLP learn the node representation and apply a score function on the focal node
 645 pair to represent the link. As GAE-like models are not implemented in the fashion of subgraph link
 646 prediction, the subgraph extraction step is necessary for them as preprocessing. We follow the code
 647 from the labeling trick [19], which implements the GAE models as the subgraph link prediction
 648 task. In particular, GIN concatenates the node embedding from different layers to learn the node
 649 representation and applies a subgraph-level readout to aggregate as the subgraph representation.

650 For the selection of hyperparameters, we use the same configuration as [19] on datasets Cora, Citeseer
 651 and Pubmed. As they do not have experiments on other 8 networks without attributes, we set the
 652 subgraph hop number as 2 and leave the rest of them as default. For PLNLP, we also add a subgraph
 653 extraction step without modifying the core part of the pairwise learning strategy. Then, we find that
 654 the performance of PLNLP is very unstable on different train/test splits. The performance’s standard
 655 deviation of PLNLP is over 10% on each experiment. Therefore, we apply the Double-Radius Node
 656 Labeling [11] to stabilize the model.

657 SEAL and WalkPool have applied one of the FakeEdge techniques in their initial implementation.
 658 SEAL uses a *Edge Minus* strategy to remove all the edges at focal node pair as a preprocessing step,
 659 while WalkPool applies *Edge Plus* to always inject edges into the subgraph for node representation
 660 learning. Additionally, WalkPool has the walk-based pooling method operating on both the *Edge*
 661 *Plus* and *Edge Minus* graphs. This design is kept in our experiment. Thus, our FakeEdge technique
 662 only takes effect on the node representation step for WalkPool. From the results in Section 5.2, we
 663 can conclude that the dataset shift issue on the node representation solely would significantly impact
 664 the model performance. We also use the same hyperparameter settings as originally reported in their
 665 paper. The code will be publicly available.

666 E Benchmark dataset descriptions

667 The graph datasets with node attributes are three citation networks: **Cora** [44], **Citeseer** [45] and
 668 **Pubmed** [46]. Nodes represent publications and edges represent citation links. The graph datasets
 669 without node attributes are: (1) **USAir** [47]: a graph of US Air lines; (2) **NS** [48]: a collaboration
 670 network of network science researchers; (3) **PB** [49]: a graph of links between web pages on US
 671 political topic; (4) **Yeast** [50]: a protein-protein interaction network in yeast; (5) **C.ele** [51]: the
 672 neural network of *Caenorhabditis elegans*; (6) **Power** [51]: the network of the western US’s electric
 673 grid; (7) **Router** [52]: the Internet connection at the router-level; (8) **E.coli** [53]: the reaction network
 674 of metabolites in *Escherichia coli*. The detailed statistics of the datasets can be found in Table 3.

Table 3: Statistics of link prediction datasets.

Dataset	#Nodes	#Edges	Avg. node deg.	Density	Attr. Dimension
Cora	2708	10556	3.90	0.2880%	1433
Citeseer	3327	9104	2.74	0.1645%	3703
Pubmed	19717	88648	4.50	0.0456%	500
USAir	332	4252	12.81	7.7385%	-
NS	1589	5484	3.45	0.4347%	-
PB	1222	33428	27.36	4.4808%	-
Yeast	2375	23386	9.85	0.8295%	-
C.ele	297	4296	14.46	9.7734%	-
Power	4941	13188	2.67	0.1081%	-
Router	5022	12516	2.49	0.0993%	-
E.coli	1805	29320	16.24	1.8009%	-

Table 4: Comparison with and without FakeEdge (Hits@20). The best results are highlighted in bold.

Models	FakeEdge	Cora	Citeseer	Pubmed	USAir	NS	PB	Yeast	C.ele	Power	Router	E.coli
GCN	<i>Original</i>	65.35±3.64	61.71±2.60	48.97±1.92	87.69±3.92	92.77±1.72	41.60±2.52	85.26±1.90	65.33±7.55	39.64±5.47	39.41±2.38	82.21±2.02
	<i>Edge Plus</i>	68.31±2.89	65.80±3.28	55.70±3.07	89.34±4.09	93.28±1.69	43.98±6.25	87.19±2.13	66.68±5.25	46.92±3.78	72.03±2.85	86.03±1.40
	<i>Edge Minus</i>	67.97±2.62	66.13±3.30	54.29±2.66	90.57±3.30	93.61±1.68	43.92±5.82	86.66±2.18	66.07±6.14	47.97±2.58	72.34±2.58	85.68±1.84
	<i>Edge Mean</i>	67.76±3.02	66.11±2.48	54.55±2.88	89.48±3.52	92.77±1.99	44.64±6.93	86.64±2.03	65.28±6.33	47.54±2.95	72.26±2.68	85.62±1.71
	<i>Edge Att</i>	68.43±3.72	67.65±4.11	55.55±2.70	90.80±4.50	92.88±2.27	44.80±6.60	87.83±0.92	65.93±11.06	48.50±2.20	70.96±2.85	86.56±1.69
SAGE	<i>Original</i>	61.67±3.68	61.10±1.54	45.29±3.99	89.20±2.80	91.93±2.74	39.51±4.44	84.11±1.47	58.55±7.17	42.97±5.34	30.02±2.75	75.30±2.77
	<i>Edge Plus</i>	68.58±2.77	65.47±3.58	55.23±2.81	92.59±3.71	93.83±2.54	49.10±5.38	89.36±0.72	69.72±6.02	49.70±2.57	74.90±3.73	88.16±1.29
	<i>Edge Minus</i>	66.26±2.54	62.97±3.50	53.43±3.52	91.32±3.42	93.54±1.96	48.72±4.90	88.27±1.00	69.81±5.34	47.63±1.87	56.67±7.20	87.89±1.59
	<i>Edge Mean</i>	66.74±2.71	65.96±2.62	55.21±2.84	91.51±3.49	93.25±2.88	48.89±6.14	89.30±0.72	69.21±7.17	47.54±3.52	73.89±3.50	88.05±1.62
	<i>Edge Att</i>	68.80±2.65	66.62±3.67	55.18±2.99	92.92±3.11	94.09±1.60	48.53±5.15	89.10±1.17	69.30±7.53	47.06±2.21	73.60±4.68	87.63±1.66
GIN	<i>Original</i>	55.71±4.38	51.71±4.31	40.14±3.98	86.08±3.14	90.51±3.45	38.79±5.32	79.57±1.74	54.95±5.91	41.56±1.47	55.47±4.37	77.37±2.84
	<i>Edge Plus</i>	64.42±2.67	63.56±2.92	49.75±4.50	88.68±4.10	94.85±1.90	46.17±6.12	87.58±2.22	64.49±6.52	48.59±3.33	70.67±3.58	84.13±2.12
	<i>Edge Minus</i>	63.17±2.96	63.65±4.63	50.37±4.01	89.81±1.80	94.53±2.09	45.93±6.09	88.37±2.00	67.06±11.03	47.56±1.88	71.10±1.90	83.23±2.62
	<i>Edge Mean</i>	61.46±4.64	63.74±4.20	46.97±6.49	89.86±2.62	93.98±2.88	43.48±7.74	88.16±2.11	66.73±6.79	47.66±2.91	71.09±2.68	82.48±1.99
	<i>Edge Att</i>	63.26±3.33	60.64±4.29	49.71±4.40	88.87±4.71	94.49±1.51	44.94±5.37	87.92±1.45	65.93±8.55	48.19±2.70	70.03±3.05	84.38±2.54
PLNLP	<i>Original</i>	58.77±2.59	57.21±3.91	40.03±3.46	88.87±2.75	93.76±1.65	38.90±4.38	81.17±3.54	66.36±5.65	43.52±6.47	34.61±11.29	65.68±1.56
	<i>Edge Plus</i>	66.79±2.77	67.69±4.13	44.44±14.29	95.19±1.60	95.84±1.09	45.18±4.87	88.04±2.42	71.21±8.04	52.3±3.96	75.01±1.83	84.73±1.70
	<i>Edge Minus</i>	67.40±3.53	62.84±2.88	47.80±11.11	94.10±2.42	95.22±1.60	45.40±6.29	87.94±1.64	69.91±6.80	52.19±4.23	68.24±4.01	83.59±1.56
	<i>Edge Mean</i>	68.61±3.40	64.81±3.57	51.92±13.30	95.24±2.09	95.95±0.78	45.37±5.07	88.08±2.30	71.26±8.08	51.97±3.41	74.42±2.33	84.78±1.82
	<i>Edge Att</i>	67.82±3.58	64.37±3.73	48.47±12.01	95.38±2.02	95.62±0.81	45.28±5.11	88.57±1.80	70.65±8.11	51.79±4.07	74.99±1.92	85.10±1.88
SEAL	<i>Original</i>	60.95±8.00	61.56±2.12	48.80±3.33	91.27±2.53	91.72±2.01	43.44±6.82	85.33±1.76	64.21±5.86	39.30±3.79	59.47±6.66	84.15±2.16
	<i>Edge Plus</i>	60.51±7.70	65.12±2.18	50.90±3.96	90.85±4.12	93.61±1.87	46.77±4.80	86.66±1.59	65.47±7.68	45.90±2.85	70.06±3.57	85.76±2.04
	<i>Edge Minus</i>	60.74±6.60	65.14±2.93	51.23±3.82	90.66±3.49	92.19±2.03	47.21±4.73	86.49±2.08	63.64±6.93	46.42±3.42	70.43±4.40	85.50±2.06
	<i>Edge Mean</i>	62.94±5.78	64.99±4.36	51.83±3.66	91.84±2.93	92.92±2.12	46.02±4.22	86.25±2.17	65.93±6.87	46.57±3.22	70.08±3.85	85.85±1.81
	<i>Edge Att</i>	62.03±4.95	63.52±4.39	48.42±5.69	91.42±3.31	94.64±1.49	44.73±5.29	86.83±1.63	65.93±4.74	47.91±3.45	67.46±3.49	86.02±1.58
WalkPool	<i>Original</i>	69.98±3.37	64.22±2.84	57.30±2.56	95.09±2.78	96.02±1.64	47.74±5.81	88.24±1.33	78.55±5.83	43.58±4.40	56.21±13.92	83.41±1.72
	<i>Edge Plus</i>	69.13±2.31	64.51±2.25	59.23±3.09	95.00±3.09	96.06±1.65	46.18±5.40	89.79±0.70	78.36±5.30	56.27±4.17	77.65±2.83	86.44±1.52
	<i>Edge Minus</i>	69.34±2.45	64.26±1.93	59.44±3.10	95.14±2.93	95.99±1.67	46.79±4.88	89.57±0.85	77.90±4.49	55.72±3.63	77.62±2.64	87.24±0.77
	<i>Edge Mean</i>	70.27±2.96	62.84±4.79	59.85±3.84	95.24±2.45	95.17±1.63	46.27±5.00	89.58±0.91	77.94±4.55	56.18±3.74	76.88±2.76	86.89±1.84
	<i>Edge Att</i>	69.60±4.11	64.35±3.64	59.63±3.28	95.61±2.53	96.06±1.62	46.77±5.36	89.84±0.71	77.94±4.89	56.46±3.55	76.90±2.82	87.02±1.64

675 F Results measured by Hits@20 and statistical significance of results

676 We adopt another widely used metrics in the link prediction task [59], Hits@20, to evaluate the model
677 performance with and without FakeEdge. The results are shown in Table 4. FakeEdge can boost all
678 the models predictive power on different datasets.

Table 5: p -values by comparing AUC scores with *Original* and *Edge Att*. Significant differences are highlighted in bold.

Models	Cora	Citeseer	Pubmed	USAir	NS	PB	Yeast	C.ele	Power	Router	E.coli
GCN	$3.50 \cdot 10^{-09}$	$6.92 \cdot 10^{-12}$	$1.52 \cdot 10^{-09}$	$1.10 \cdot 10^{-05}$	$9.89 \cdot 10^{-04}$	$1.21 \cdot 10^{-09}$	$4.95 \cdot 10^{-13}$	$2.76 \cdot 10^{-01}$	$1.55 \cdot 10^{-05}$	$2.62 \cdot 10^{-13}$	$2.44 \cdot 10^{-14}$
SAGE	$1.32 \cdot 10^{-08}$	$2.04 \cdot 10^{-06}$	$3.48 \cdot 10^{-14}$	$2.78 \cdot 10^{-02}$	$2.33 \cdot 10^{-02}$	$4.13 \cdot 10^{-06}$	$4.87 \cdot 10^{-08}$	$1.23 \cdot 10^{-03}$	$6.12 \cdot 10^{-10}$	$4.40 \cdot 10^{-12}$	$3.54 \cdot 10^{-13}$
GIN	$4.86 \cdot 10^{-10}$	$6.09 \cdot 10^{-11}$	$1.46 \cdot 10^{-12}$	$1.27 \cdot 10^{-03}$	$1.29 \cdot 10^{-05}$	$2.47 \cdot 10^{-10}$	$5.34 \cdot 10^{-11}$	$3.84 \cdot 10^{-04}$	$5.10 \cdot 10^{-09}$	$3.11 \cdot 10^{-16}$	$3.04 \cdot 10^{-11}$
PLNLP	$1.47 \cdot 10^{-10}$	$5.30 \cdot 10^{-07}$	$1.22 \cdot 10^{-06}$	$1.66 \cdot 10^{-07}$	$1.70 \cdot 10^{-02}$	$3.40 \cdot 10^{-08}$	$7.69 \cdot 10^{-06}$	$2.46 \cdot 10^{-03}$	$7.84 \cdot 10^{-06}$	$2.68 \cdot 10^{-13}$	$5.27 \cdot 10^{-11}$
SEAL	$2.59 \cdot 10^{-01}$	$1.72 \cdot 10^{-02}$	$6.45 \cdot 10^{-05}$	$4.82 \cdot 10^{-01}$	$1.15 \cdot 10^{-01}$	$5.20 \cdot 10^{-01}$	$5.91 \cdot 10^{-04}$	$4.12 \cdot 10^{-01}$	$3.78 \cdot 10^{-06}$	$3.91 \cdot 10^{-06}$	$5.67 \cdot 10^{-04}$
WalkPool	$9.52 \cdot 10^{-01}$	$4.96 \cdot 10^{-01}$	$2.83 \cdot 10^{-07}$	$4.77 \cdot 10^{-01}$	$8.91 \cdot 10^{-01}$	$1.84 \cdot 10^{-05}$	$1.07 \cdot 10^{-04}$	$8.74 \cdot 10^{-01}$	$4.15 \cdot 10^{-07}$	$5.89 \cdot 10^{-04}$	$1.83 \cdot 10^{-10}$

Table 6: Model performance with only 20% training data (AUC). The best results are highlighted in bold.

Models	Fake Edge	Cora	Citeseer	Pubmed	USAir	NS	PB	Yeast	C.ele	Power	Router	E.coli
GCN	<i>Original</i>	55.02±1.00	56.34±0.73	57.09±1.46	80.44±1.43	61.23±1.22	88.52±0.37	81.12±0.52	66.67±2.34	49.15±0.56	62.98±8.98	81.79±0.76
	<i>Edge Att</i>	63.27±1.20	62.17±0.92	85.55±0.29	88.19±1.27	61.86±1.75	92.57±0.25	85.54±0.34	70.27±1.44	52.37±1.49	77.45±0.63	91.60±0.33
SEAL	<i>Original</i>	59.00±1.79	59.11±0.76	77.93±2.12	87.21±1.29	62.54±1.15	91.29±0.26	83.18±0.91	69.12±1.30	51.01±0.87	71.88±1.42	90.86±0.40
	<i>Edge Att</i>	62.11±1.67	62.08±0.60	85.11±0.50	87.74±0.83	63.66±1.54	91.92±0.35	85.62±0.54	68.89±1.35	52.99±1.02	77.78±0.49	91.06±0.34

Note that the AUC scores on several datasets are almost saturated in Table 1. To further verify the statistical significance of the improvement, a two-sided t -test is conducted with the null hypothesis that the augmented *Edge Att* and the *Original* representation learning would reach at the identical average scores. The p -values of different methods can be found in Table 5. Recall that the p -value smaller than 0.05 is considered as statistically significant. GAE-like methods obtain significant improvement on almost all of the datasets, except GCN on C.ele. SEAL shows significant improvement with *Edge Att* on 7 out of 11 datasets. For WalkPool, more than half of the datasets are significantly better.

G FakeEdge with extremely sparse graphs

In real applications, the size of testing set often outnumbers the training set. When it happens to a link prediction task, the graph will become more sparse because of the huge number of unseen links. We are interested to see how FakeEdge can handle situations where the ratio of training set is low and there exists a lot of “true” links missing in the training graph.

We reset the train/test split as 20% for training, 30% for validation and 50% for testing and reevaluate the model performance. The results can be found in Table 6. As shown in the table, FakeEdge can still consistently improve the model performance under such an extreme setting. It shows that the dataset shift for link prediction is a common issue and FakeEdge has the strength to alleviate it in various settings.

However, we still observe a significant performance drop when compared to the 85/5/10 evaluation setting. This degradation may be caused by a more fundamental dataset shift problem of link prediction: the nodes in a graph are not sampled independently. Existing link prediction models often assume that the likelihood of forming a link relies on its local neighborhood. Nevertheless, an intentionally-sparsified graph can contain a lot of missing links from the testing set, leading to corrupted local neighborhoods of links which cannot reflect the real environments surrounding. FakeEdge does not have the potential to alleviate such a dataset shift. We leave this as a future work.

H Concatenation as another valid Edge Invariant subgraph embedding

Edge Concat To fuse the feature from *Edge Plus* and *Edge Minus*, another simple and intuitive way is to concatenate two embedding into one representation. Namely, $\mathbf{h}^{concat} = [\mathbf{h}^{plus}; \mathbf{h}^{minus}]$, where $[\cdot; \cdot]$ is the concatenation operation. \mathbf{h}^{concat} is also an Edge Invariant subgraph embedding. In Table 7, we observe that *Edge Concat* has the similar performance improvement like other FakeEdge methods on all different backbone models.

I Heuristic methods with FakeEdge

FakeEdge, as a model-agnostic technique, not only has the capability of alleviating the dataset shift issue for GNN-based models, but also can tackle the problem for heuristic methods. Some of the conventional heuristic link predictors, like Common Neighbor [1], Adamic–Adar index [20], or Resource Allocation [39], are Edge Invariant because these predictors are independent of the existence of the target link.

However, other link predictors, including Preferential Attachment (PA) [37] and Jaccard Index (Jac) [38], are not Edge Invariant. The existence/absence of target link can change the values of

Table 7: Comparison for concatenation operation (AUC). The best results are highlighted in bold.

Models	Fake Edge	Cora	Citeseer	Pubmed	USAir	NS	PB	Yeast	C.cele	Power	Router	E.coli
GCN	<i>Original</i>	84.92±1.95	77.05±2.18	81.58±4.62	94.07±1.50	96.92±0.73	93.17±0.45	93.76±0.65	88.78±1.85	76.32±4.65	60.72±5.88	95.35±0.36
	<i>Edge Att</i>	92.06±0.85	88.96±1.05	97.96±0.12	97.20±0.69	97.96±0.39	95.46±0.45	97.65±0.17	89.76±2.06	85.26±1.32	95.90±0.47	98.04±0.16
	<i>Edge Concat</i>	92.63±1.00	89.88±1.00	97.96±0.11	97.27±0.95	98.07±0.78	95.39±0.44	97.55±0.46	89.78±1.59	85.71±0.75	96.19±0.59	98.06±0.23
SAGE	<i>Original</i>	89.12±0.90	87.76±0.97	94.95±0.44	96.57±0.57	98.11±0.48	94.12±0.45	97.11±0.31	87.62±1.63	79.35±1.66	88.37±1.46	95.70±0.44
	<i>Edge Att</i>	93.31±1.02	91.01±1.14	98.01±0.13	97.40±0.94	98.70±0.59	95.49±0.49	98.22±0.24	90.64±1.88	86.46±0.91	96.31±0.59	98.43±0.13
	<i>Edge Concat</i>	93.03±0.57	91.14±1.46	98.08±0.07	97.54±0.70	98.59±0.26	95.66±0.39	98.04±0.37	91.14±1.19	86.46±1.04	96.19±0.54	98.40±0.22
GIN	<i>Original</i>	82.70±1.93	77.85±2.64	91.32±1.13	94.89±0.89	96.05±1.10	92.95±0.51	94.50±0.65	85.23±2.56	73.29±3.88	84.29±1.20	94.34±0.57
	<i>Edge Att</i>	90.76±0.88	89.55±0.61	97.50±0.15	96.34±0.82	98.35±0.54	95.29±0.29	97.66±0.33	89.39±1.61	86.21±0.67	95.78±0.52	97.74±0.33
	<i>Edge Concat</i>	90.90±0.92	89.94±0.89	97.48±0.16	96.17±0.64	98.41±0.73	95.45±0.39	97.71±0.38	88.81±1.41	86.77±0.99	95.72±0.47	97.72±0.18
PLNLP	<i>Original</i>	82.37±1.70	82.93±1.73	87.36±4.90	95.37±0.87	97.86±0.93	92.99±0.71	95.09±1.47	88.31±2.21	81.59±4.31	86.41±1.63	90.63±1.68
	<i>Edge Att</i>	91.22±1.34	88.75±1.70	98.41±0.17	98.13±0.61	98.70±0.40	95.32±0.38	98.06±0.37	91.72±2.12	90.08±0.54	96.40±0.40	98.01±0.18
	<i>Edge Concat</i>	93.01±1.16	91.19±1.52	98.45±0.12	97.86±0.37	98.81±0.33	95.18±0.24	98.04±0.21	91.79±1.79	89.16±1.01	96.31±0.36	98.13±0.18
SEAL	<i>Original</i>	90.13±1.94	87.59±1.57	95.79±0.78	97.26±0.58	97.44±1.07	95.06±0.46	96.91±0.45	88.75±1.90	78.14±3.14	92.35±1.21	97.33±0.28
	<i>Edge Att</i>	91.08±1.67	89.35±1.43	97.26±0.45	97.04±0.79	98.52±0.57	95.19±0.43	97.70±0.40	89.37±1.40	85.24±1.39	95.14±0.62	97.90±0.33
	<i>Edge Concat</i>	90.22±1.60	89.93±1.31	97.40±0.24	96.83±1.01	98.23±0.49	95.29±0.43	97.68±0.34	88.99±1.13	85.60±1.03	95.76±0.74	97.72±0.25
WalkPool	<i>Original</i>	92.00±0.79	89.64±1.01	97.70±0.19	97.83±0.97	99.00±0.45	94.53±0.44	96.81±0.92	93.71±1.11	82.43±3.57	87.46±7.45	95.00±0.90
	<i>Edge Att</i>	91.98±0.80	89.36±0.74	98.37±0.19	98.12±0.81	99.03±0.50	95.47±0.27	98.28±0.24	95.63±1.11	91.25±0.60	97.27±0.27	98.70±0.14
	<i>Edge Concat</i>	91.77±1.06	89.79±0.87	98.48±0.09	98.07±0.86	99.05±0.44	95.46±0.35	98.30±0.25	93.82±1.09	91.29±0.77	97.31±0.27	98.70±0.17

Table 8: Heuristic methods with/without FakeEdge (AUC). The best results are highlighted in bold.

Models	Fake Edge	Cora	Citeseer	Pubmed	USAir	NS	PB	Yeast	C.cele	Power	Router	E.coli
PA	<i>Original</i>	63.15±1.38	58.20±2.18	71.72±0.36	88.84±1.41	66.19±1.82	90.05±0.52	82.10±1.15	75.72±2.20	44.47±1.58	48.20±0.83	91.99±0.78
	<i>Edge Plus</i>	65.05±1.31	61.05±1.96	84.04±0.37	90.36±1.45	65.29±1.97	90.47±0.49	82.66±0.98	75.98±2.31	46.83±1.61	74.03±1.05	91.98±0.78
	<i>Edge Minus</i>	63.15±1.38	58.20±2.18	71.72±0.36	88.84±1.41	66.19±1.82	90.05±0.52	82.10±1.15	75.72±2.20	44.47±1.58	48.20±0.83	91.99±0.78
Jac	<i>Original</i>	71.76±0.85	66.33±1.23	64.41±0.20	88.89±1.55	92.19±0.80	86.82±0.60	88.49±0.53	78.77±1.94	58.18±0.50	55.77±0.55	81.43±0.92
	<i>Edge Plus</i>	71.77±0.85	66.33±1.23	64.42±0.20	89.65±1.45	92.19±0.80	87.20±0.58	88.52±0.53	79.33±1.88	58.18±0.50	55.77±0.55	81.79±0.90
	<i>Edge Minus</i>	71.76±0.85	66.33±1.23	64.41±0.20	88.89±1.55	92.19±0.80	86.82±0.60	88.49±0.53	78.77±1.94	58.18±0.50	55.77±0.55	81.43±0.92

the predictors. Following the protocol in the previous experiment, we apply FakeEdge on such link predictors to evaluate if the dataset shift issue can also be mitigated. The results are shown in Table 8.

As shown in the table, FakeEdge can significantly improve the performance of the PA predictor on several datasets. With FakeEdge, PA performs over 10% better on Pubmed. Surprisingly, even though PA is not able to predict the links on Router dataset with AUC score lower than 50%, PA with Edge Plus achieves 74% AUC score and becomes a functional link predictor. In terms of Jac, we observe that Jac with FakeEdge can only gain marginal improvement. Even though Jac is dependent on the existence of target link, its change is relatively small when the existence of the target link flips.

J Dataset shift vs expressiveness: which contributes more with FakeEdge?

In Section 4.3, we discussed how FakeEdge can enhance the expressive power of GNN-based models on non-isomorphic focal node pairs. Meanwhile, we have witnessed the boost of model performance brought by FakeEdge in the experiments. One natural question to ask is whether resolving the dataset shift issue or lifting up expressiveness contributes more to make the model perform better.

To answer the question, we first revisit the condition of achieving greater expressiveness. FakeEdge will lift up the expressive power when there exists two nodes being isomorphic in the graph, where we can construct a pair of non-isomorphic focal node pairs which GNNs cannot distinguish. Therefore, how often such isomorphic nodes exist in a graph will determine how much improvement FakeEdge can make by bringing greater expressiveness. Even though isomorphic nodes are common in specific types of graphs like regular graphs, it can be rare in the real world datasets [60]. Thus, we tend to conclude that the effect of solving dataset shift issue by FakeEdge contributes more to the performance improvement rather than greater expressive power. But fully answering the question needs a further rigorous study.

K Limitation

FakeEdge can align the embedding of isomorphic subgraphs in training and testing sets. However, it can pose a limitation that hinders one aspect of the GNN-based model’s expressive power. Figure 1 gives an example where subgraphs are from training and testing phases, respectively. Now consider that those two subgraphs are both from training set ($c = \text{train}$). Still, the top subgraph has edge observed at focal node pair ($y = 1$), while the other does not ($y = 0$). With FakeEdge, two

749 subgraphs will be modified to be isomorphic, yielding the same representation. However, they are
750 non-isomorphic before the modification. To the best of our knowledge, no existing method can
751 simultaneously achieve the most expressive power and get rid of dataset shift issue, because the edge
752 at the focal node pair in the testing set can never be observed under a practical problem setting.